

https://africanjournalo@iomedicalresearch.com/index.php/AJBR

Afr. J. Biomed. Res. Vol. 28(3s) (June 2025); 591-615
Research Article

The Ability to Inhibit A-Amylase And A-Glucosidase by Aromatic Compounds in Cinnamomi Ramulus Extract: An in-Silico Investigation

Nguyen Thi Thanh Thao¹, Vo Van On^{1*}, Kiet Ho¹, Nguyen Thi Lien Thuong¹,
Phan Van Huan²

¹Institute of Innovation in Pharmaceutical and HealthCare Food, Thu Dau Mot University, Binh Duong
Province, Vietnam, Email: thuongntl@tdmu.edu.vn

^{2*} Faculty of Basic Science, Binh Duong University, Binh Duong Province, Viet Nam

*Corresponding Author: Vo Van On *Email: onvv@tdmu.edu.vn thuongntl@tdmu.edu.vn

ABSTRACT

This study investigates the potential inhibitory effects of 13 aromatic compounds found in ramulus cinnamomi extract against α -amylase (AA) and α -glucosidase (AG) enzymes, which play crucial roles in carbohydrate metabolism and are important therapeutic targets for type 2 diabetes management. Through molecular docking simulations, pharmacokinetic analysis, and toxicity assessments, we compared these compounds with established inhibitors including acarbose, voglibose, and miglitol. The molecular docking results revealed that benzyl benzoate demonstrated superior binding energies (-6.819 kcal/mol for AA and -6.897 kcal/mol for AG) compared to other tested compounds and showed comparable or better interaction profiles than the reference drugs. Detailed analysis of protein-ligand interactions showed that while reference drugs primarily formed hydrogen bonds, the aromatic compounds exhibited predominantly hydrophobic interactions, suggesting a distinct mechanism of inhibition. Pharmacokinetic studies indicated favorable drug-like properties for most compounds, particularly benzyl benzoate, with high gastrointestinal absorption and bloodbrain barrier permeability. Although the investigated compounds showed higher acute toxicity than reference drugs, their LD50 values remained within acceptable ranges for therapeutic development. These findings suggest that aromatic compounds from ramulus cinnamomi, especially benzyl benzoate, represent promising candidates for developing new type 2 diabetes treatments through dual inhibition of AA and AG enzymes.

*Author of correspondence: Email: onvv@tdmu.edu.vn

Received -15/05/2025 Accepted - 27/05/2025

DOI: https://doi.org/10.53555/AJBR.v28i3S.7960

© 2025 The Author(s).

This article has been published under the terms of Creative Commons Attribution-Noncommercial 4.0 International License (CC BY-NC 4.0), which permits noncommercial unrestricted use, distribution, and reproduction in any medium, provided that the following statement is provided. "This article has been published in the African Journal of Biomedical Research"

1. INTRODUCTION

79, living with diabetes worldwide, of which 81% of

Diabetes is a chronic metabolic condition characterized by excessive blood sugar levels, which cause damage to numerous organs in the body. According to statistics in 2021 from the International Diabetes Federation (IDF)[1], there are about 537 million adults, aged 20 to patients are mainly distributed in low- and middle-income countries. Worryingly, up to 44% of patients are not diagnosed in advance, leading to more difficult treatment when the disease has entered a severe stage. Forecasts show that patients may increase to 643 million by 2030 and about 784 million by 2045. In 2021, the number of fatalities from diabetes reached 6.7 million

cases. The total cost of diabetes care globally in 2021 is estimated at US\$966 billion. The Western Pacific area has the most people living with diabetes, with 206 million cases in 2021, and is anticipated to climb to 238 million by 2030 and 260 million by 2045. Based on the IDF's 2021 report, the African area has the fewest individuals living with diabetes, with roughly 24 million cases; approximately half of them are undiagnosed, with around 12.7 million cases.

Type 2 diabetes, which accounts for 90% of all diabetes cases worldwide[1], usually occurs in adults when the body becomes resistant to insulin, making this hormone gradually less effective, and forcing the endocrine organs to increase insulin production to supply life processes. Over time, when the demand for insulin increases beyond the secretory capacity of the pancreatic β cells, these β cells become exhausted and die, leading to severe insulin deficiency in the body[2]. Some common recommendations are given to control the symptoms and complications of type 2 diabetes such as healthy diet, exercise, not smoking, weight control... Additionally, several medicines are used to regulate blood sugar levels, such as metformin[3], approved by the FDA in 1995; sulfonylureas: glyburide and glipizide, used in combination with metformin[4, 5]; dipeptidyl peptidase-4 (DPP-4) inhibitors[6] such as sitagliptin[7], saxagliptin[8], linagliptin[9], alogliptin[10]; GLP-1 receptor inhibitors: liraglutide[11], semaglutide[12], dulaglutide[13], tirzepatide[14]; sodium-glucose cotransporter-2 (SGLT2): dapagliflozin[15], canagliflozin[16], empagliflozin[17], ertugliflozin[18]. Besides that, experts also pay attention to work on limiting blood sugar at the source, including research and development of inhibitors for the enzymes αamylase and α -glucosidase[19-21]. The α -amylase and α-glucosidase are the enzymes that play a key role in carbohydrate metabolism[22, 23]. The α -amylase hydrolyzes the α -1,4-glycosidic bonds of starch to form shorter oligosaccharides such as maltose and dextrins, while α -glucosidase completes the conversion to glucose for absorption across the intestinal wall into the blood[24, 25]. Simultaneous inhibition of both enzymes is considered a potential therapeutic strategy for type 2 diabetes[26, 27]. Several inhibitors of these two enzymes have been licensed, such as acarbose[28], voglibose[29], and miglitol[30], which mainly compete with the substrates of α -amylase and α -glucosidase.

Recent studies have shown that plant polyphenols are effective inhibitors of both these enzymes[31, 32]. Some reports have identified several flavonoids with dual inhibitory activity against both α -amylase and α -glucosidase[33, 34]. Several other bioactive compounds such as lupenone, baicalein, and ursolic acid have been found to have α -glucosidase inhibitory potential[35, 36]. In the research for natural agents capable of inhibiting α -amylase and α -glucosidase enzymes, cinnamon (Cinnamomum spp.) has emerged as a promising candidate[37, 38]. Experiments have revealed that cinnamon not only enhances insulin sensitivity but also decreases blood glucose levels through numerous pathways[39, 40]. In particular, typical compounds in cinnamon, such as cinnamaldehyde (accounting for 65-

80%) along with eugenol and coumarin derivatives, have been shown to have many valuable biological activities such as anti-oxidation, anti-inflammation and blood glucose regulation[41, 42].

Advances in computational technology have greatly facilitated screening studies as well as understanding the mechanisms of interactions between natural compounds and enzymes[43, 44]. Ogboye et al. reported several compounds extracted from selected Nigerian plants that have the potential to inhibit two enzymes α -amylase and α -glucosidase by using docking, ADMET, and molecular dynamics simulation[45]. Sharma et al. used MD simulation to identify six natural compounds from herbs that have the potential to inhibit α -amylase[46]. Riyaphan and others with the support of in silico methods such as docking, QSAR to identify polyphenol active ingredients to inhibit α -glucosidase and α -amylase[47].

In a work by Jia Liu and colleagues[48], the authors introduced the compounds found in cinnamomi ramulus and their chemical-pharmaceutical properties. Among the 121 compounds described, we selected a rather special group of compounds, the group of 13 aromatic compounds in cinnamon essential oil, for investigation because (1) their molecular mass is quite small, (2) each compound is characterized by containing at least one aromatic ring. The study of aromatic compounds in cinnamon essential oil is a promising approach due to their molecular structural properties. In addition to having low molecular weight and possessing at least one aromatic ring, these compounds also exhibit diverse biological activities such as anti-inflammatory, antibacterial and antioxidant activities[49, 50]. This opens up the potential for wide application in the development of new pharmaceuticals. However, although many studies have been conducted on the inhibitory ability of cinnamon's compounds, the detailed molecular mechanism of interaction between specific compounds and enzyme active sites has not been fully elucidated. Therefore, we conducted molecular docking simulation studies to predict the interaction of these compounds with two enzymes α-amylase and αglucosidase. At the same time, the pharmacokinetic properties, the ability to penetrate biological membranes and the acute toxicity of these aromatic compounds were also clarified. The results obtained will be an important basis for guiding the structure optimization and the development of derivatives with better activity in the future to combat type 2 diabetes.

2. MATERIALS AND METHODS

2.1. Receptors and ligands preparation

2.1.1. Human pancreatic α-amylase

The wild-type configuration of human pancreatic α -amylase was retrieved and downloaded from the Protein Data Bank (RCSB-PDB, https://www.rcsb.org/)[51, 52] with PDB ID 4W93[53]. Overall, the 4W93 profile consists of 496 residues organized into three main domains: domain A, including residues 1-99 and 169-404, has a characteristic structure containing a barrel of eight parallel β -strands in the center surrounded by α -helices; domain B, from residues 99 to 168, forms a large

loop; and domain C (residues 405-496) has a β-sandwich structure, formed by antiparallel β-strands[54]. Domain A is the largest and most important part because it contains the catalytic site of α-amylase (AA), which is well defined with three important residues: Glu233 (plays a role as acid/base catalyst), Asp197 (nucleophile) and Asp300 (stabilizer). Residue Glu233, at the beginning of hydrolysis, acts as an acid, donating a proton to the oxygen atom of the glycosidic bond, and facilitating bond cleavage. In the later step, it switches to the base role, taking a proton from a water molecule, promoting the hydrolysis reaction. Meanwhile residue Asp197 attacks the anomeric carbon (C1) of the sugar molecule, forming a temporary covalent bond with the substrate. The formation of this intermediate enzymesubstrate complex is a key step in the conformational retention mechanism of the hydrolysis reaction. Simultaneously, residue Asp300 interacts with the hydroxyl group at the C2 position of the sugar in the -1 subsite, helping to orient the substrate and stabilize the transition state of the reaction[55]. In addition, the 4W93 conformation contains two ions in the active site, Ca2+ and Cl- ions. The position of the Ca2+ ion is located at the interface between domains A and B coordinated by residues Asn100, Arg158, Asp167, and His201. This position is highly conserved in the α -amylase family and plays an essential role in maintaining the active conformation of the enzyme. The Cl- ion is located at the area formed by residues Arg195, Asn298 and Arg337[55]. The substrate-binding region consists of subsites from -4 to +2, in which residues Tyr56, Trp57, Tvr151, and His299 form the -1 subsite, where glycosidic bond cleavage occurs. Li et al. (2013) showed that residues Trp178, Tyr151, and His305 play important roles in substrate orientation and stabilization. The enzyme also has a proline-rich surface region (residue 401-417) that plays a role in stabilizing the structure under acidic conditions. The cysteine residues at positions Cys150-Cys164, Cys240-Cys283,

Cys399-Cys470 form disulfide bridges, contributing to the three-dimensional stability of the enzyme. The secondary structural elements are distributed as follows: 42% α -helix (mainly in domain A), 20% β -sheet (concentrated in domain C), and the remainder are irregular structures and loops. These structures are stabilized by a network of hydrogen bonds and hydrophobic interactions in the protein core. (See Figure 1)

2.1.2. Lysosomal acid-a-glucosidase

The lysosomal acid-α-glucosidase (AG) structure used, with PDB ID 5NN4, has a total of 872 amino acids and organized into several distinct functional domains[56]. According to Sugawara's group (2009), the structure of a human acid-α-glucosidase is composed of five domains[57]. Containing amino acids 89 to 135 is the trefoil type-P domain that regulates enzyme activity through interactions with sugar molecules. The Nterminal beta-sheet domain, determined from amino acids 136 to 346, is involved in the recognition and binding of the glycogen substrate[58]. The catalytic domain, comprising amino acids 347 to 723, contains the enzyme's active site, where the hydrolysis of α -1,4 and α -1,6 glycosidic bonds of glycogen takes place [56]. The proximal C-terminal domain (amino acids 724–818) and distal C-terminal domain (amino acids 819-952) play a role in stabilizing the enzyme's structure and assisting in protein folding[59]. The active site of αglucosidase, where the glycogen degradation reaction occurs, is located deep within the GH31 catalytic domain, defined by key residues such as Asp404, Met519, Arg600, Trp613, Asp616, Asp645, Phe649, and His674[60]. In addition, Asp282 and Arg600 participate in substrate recognition and stabilization, enabling Asp518 and Asp616 to act as nucleophilic and acid/base catalysts[59]. (See Figure 2)

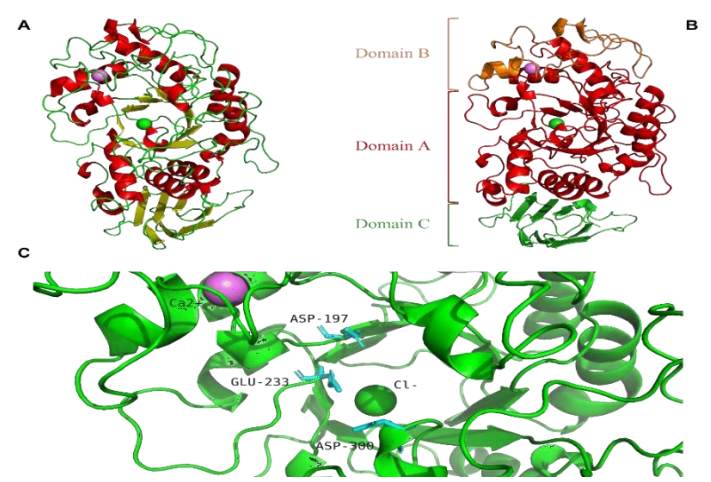


Figure 1: Illustration of the 3D structure of α-amylase (AA), PDB ID 4W93. (A) The secondary structure of AA is in which violet atom is a calcium ion, and green atom is a chloride ion. (B) Three primary domains of AA include domain A (from residue 1 to 99 and residue 169-404; red part), domain B (from residue 99 to 168; orange part) and domain C (from residue 405 to 496; green part). (C) The active site of AA that is determined based on three residues: Asp197, Glu233 and Asp300 (cian objects).

594

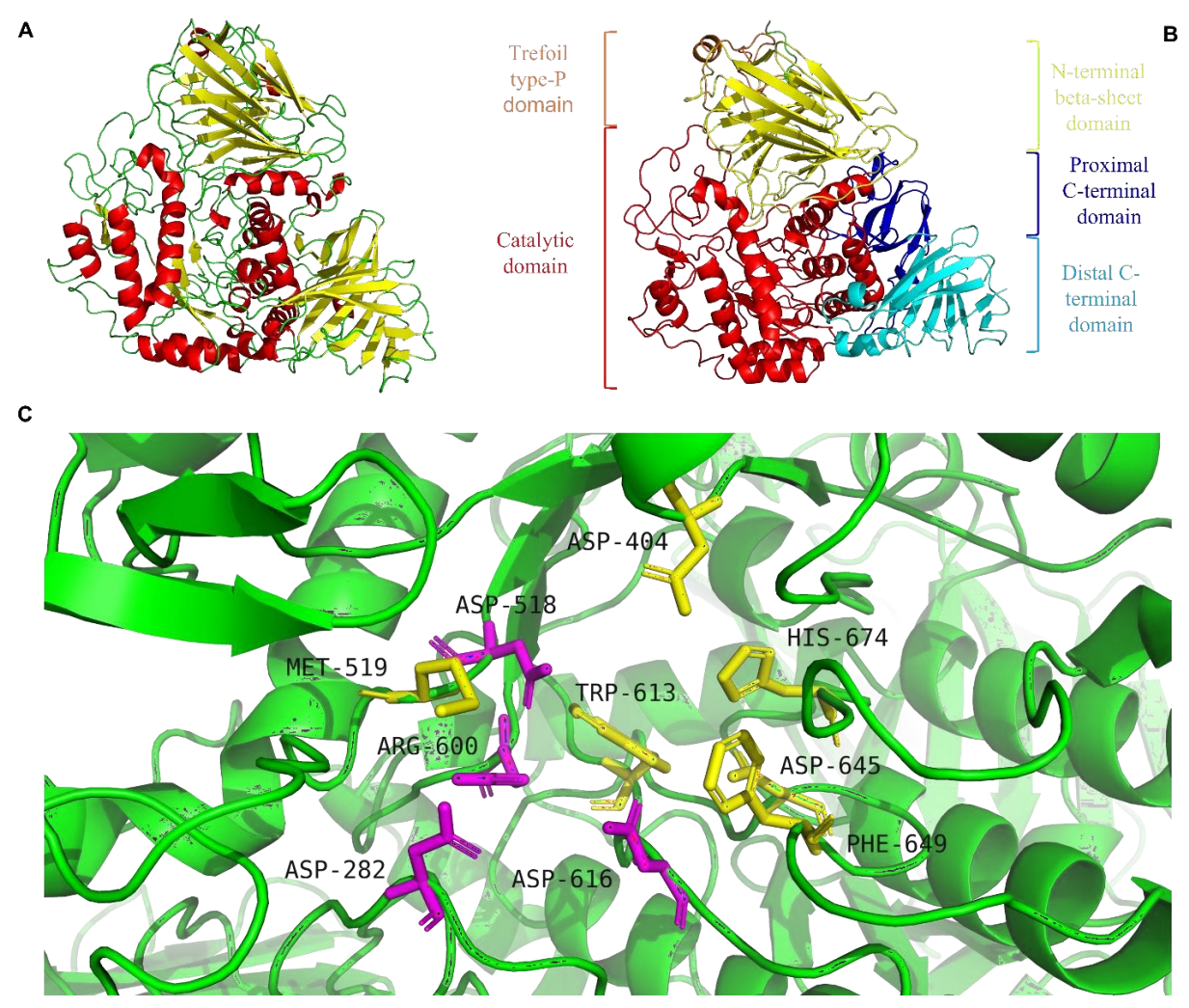


Figure 2: Illustration of the 3D structure of α-glucosidase (AG), PDB ID 5NN4. (A) The secondary structure of AG. (B) Five main domains of AG include trefoil type-P domain (from residue 136 to 346; orange part), N-terminal beta-sheet domain (from residue 136 to 346; yellow part), catalytic domain (from residue 347 to 723; red part), proximal C-terminal domain (from residue 724 to 818; blue part) and distal C-terminal domain (from residue 819 to 952; cian part). (C) The active site of AG that is determined based on several residues as Asp404, Met519, Arg600, Trp613, Asp616, Asp645, Phe649 and His674; in which Asp282, Asp518, Arg600 and Asp616 are directly involved in the hydrolysis of the substrate.

2.1.3. Ligands preparation

We chose to examine 13 aromatic compounds extracted from cinnamomi ramulus, from the publication of Liu et al. 2020[48]. These compounds are relatively small in size, with the number of atoms of each substance being less than 30 atoms. The characteristic of these 13 compounds is that they all contain at least 1 benzene ring. The 3D structures were retrieved from the PubChem database (https://pubchem.ncbi.

nlm.nih.gov/), see Table 1 for details. In addition, we also selected three control compounds, which are commercially used pharmaceutical compounds recognized by the FDA or approved in some countries, including: acarbose (FDA-approved in 1995), voglibose (approved in Japan, 1994) and miglitol (FDA-approved in 1996). The 3D molecular structures of these three reference compounds were also downloaded from the Pubchem database and their information is presented in **Table 1**.

Table 1: Information of 13 considered aromatic compounds and 3 reference compounds: acarbose, voglibose, miglitol.

Table	Table 1: Information of 13 considered aromatic compounds and 3 reference compounds: acarbose, voglibose, miglitol.								
No.	Name Pubchem CID Chemical formula	2D structure	No.	Name Pubchem CID Chemical formula	2D structure				
1	4- hydroxybenzaldehyde 126 C ₇ H ₆ O ₂	OH	9	Phenylethyl alcohol 6054 C ₈ H ₁₀ O	OH				
2	Benzaldehyde 240 C ₇ H ₆ O	0=	10	1-phenyl-1,2- propanedione 11363 C ₉ H ₈ O ₂	O ————————————————————————————————————				
3	Acetophenone 7410 C ₈ H ₈ O	O	11	1-naphthalenol 7005 C ₁₀ H ₈ O	OH				
4	Anisole 7519 C ₇ H ₈ O	0-	12	$\begin{array}{c} \text{1-} \\ \text{methylethylbenzene} \\ \text{7406} \\ \text{C}_9\text{H}_{12} \end{array}$					
5	3-phenylpropanal 7707 C ₉ H ₁₀ O	0=	13	Trans-anethole 637563 C ₁₀ H ₁₂ O					
6	Benzyl benzoate 2345 C ₁₄ H ₁₂ O ₂		14	Acarbose 41774 C ₂₅ H ₄₃ NO ₁₈	HO OH HO OH HO OH HO OH				

7	2- methylbenzaldehyde 10722 C ₈ H ₈ O	0	15	Voglibose 444020 C ₁₀ H ₂₁ NO ₇	HO OH OH
8	3- methylbenzaldehyde 12105 C ₈ H ₈ O		16	$\begin{array}{c} \text{Miglitol} \\ 441314 \\ C_8H_{17}NO_5 \end{array}$	HO N OH

2.2. Methods

2.2.1. Molecular docking simulation

AutoDockTools (ADT) software, version 1.5.7[61], was used to prepare the input for molecular docking simulation. Each receptor was added with polar hydrogens and the gasteiger's charge were calculated; and then saved in PDBQT format. The PDBQT file contains some information about the object similar to PDB formats such as atom name and order number, amino acid name, and coordinates of each atom; in addition, the file also has a column containing the value gasteiger PEOE partial charge "Q" and AutoDOCK atom type "T". The next step is to define the docking box so that this box covers the entire active region of the receptor that we need to investigate; then save the important parameters including center x, center y, center z, size x, size y, size z, and spacing grid. Specifically, for the 4W93 system, the center of gravity and the docking box dimensions are -8.167:7.750:-21.682 and 62:62:62 Å, respectively; while the parameters of the 5NN4 system are -8.993:-32.748:93.427 and 40:48:70. Both systems use a grid spacing value of 0.375. In addition, some other parameters are also specified such as exhaustiveness = 400 and the number of returned modes is 9. The ligands are also prepared through the ADT software. The software only retains the polar hydrogens on the ligand and saves the configuration in PDBQT format. The process of detecting and ranking the ligand-receptor interaction sites is performed through the Autodock Vina package, version 1.2.5[62, 63]. The output of Autodock Vina returns the coordinates and corresponding docking energies for each ligand mode in order of most negative to least negative, implying that the more negative the docking energy value, the better the interaction between the ligand and the receptor.

2.2.2. Analysis of molecular interaction

After docking, we select the best binding configuration, with the criterion that the ligand is located at the position to be investigated and has the lowest docking energy, to

extract the interactions/bonds that appear between the receptor and the ligand. The PLIP package (https://pliptool.biotec.tu-dresden.de/plip-web/plip/index) on the PYTHON environment undertakes this task. PLIP (Protein-Ligand Interaction Profiler)[64, 65] is software including both a web tool and a Linux package. That program can detect several noncovalent interactions between amino acids of the receptor and the ligand such as hydrophobic interactions, π -stacking interactions, salt-bridge interactions, hydrogen bonds, and halogen bonds.

2.2.3. Visualization tools

We used the PyMOL 2.3.0 Open-Source in Linux OS to illustrate all high resolution figures in this report. PyMOL[66] is a robust molecular graphics program that is frequently used in drug design and structural biology. Warren DeLano developed it, and Schrödinger LLC is currently in the business of maintaining it.

2.2.4. Pharmacokinetic study

In this study, we used SwissADME (http://www. swissadme.ch/index.php), a free online tool developed by the Molecular Modelling Group of the University of Lausanne and the SIB Swiss Institute of Bioinformatics[67], predict pharmacokinetic to parameters and physical-chemical properties of potential investigated compounds with development. The properties evaluated included the absorption, distribution, metabolism, and excretion (collectively referred to as ADME) of a chemical compound. The tool applies advanced in silico prediction algorithms, integrating various prediction models such as the Lipinski rule, the BOILED-Egg model[68], and other important pharmacokinetic parameters. SwissADME uses 2D structures from uploaded files or drawn directly on the website, or uses SMILES code as input for predictions, providing detailed information on gastrointestinal absorption, blood-brain barrier permeability, interactions with transport proteins such as P-glycoprotein, as well as

predictions of key cytochrome P450 drug metabolizing enzymes. The analytical approach on Swiss ADME allows for rapid and efficient screening of potential compounds' pharmacokinetic properties, contributing to optimizing the drug development process and minimizing in vitro testing costs.

2.2.5. Median lethal dose (LD50) prediction

The T.E.S.T. software (Toxicity Estimation Software (https://www.epa.gov/comptox-tools/toxicity-Tool) estimation-software-tool-test) developed by the United States Environmental Protection Agency (US EPA) provides a reliable method for estimating the acute toxicity (LD50) of chemical compounds through QSAR (Quantitative Structure-Activity Relationship) models[69]. This method is based on the analysis of the correlation between molecular structure and biological activity, using a large database of experimental toxicity. T.E.S.T. applies various prediction methods, including the nearest neighbor method, the multivariate linear regression analysis method, and the method based on molecular contribution groups. The LD50 value is estimated by combining the results from these methods, allowing the prediction of the dose that is lethal to 50% of the study population. The reliability of predictions is assessed through statistical parameters such as the correlation coefficient (R2), root mean square error (RMSE), and the model's applicability domain (AD). A model with a high R² (usually > 0.7) indicates good predictive ability. In addition, RMSE measures the average deviation between the predicted value and the experimental value, helping to evaluate the absolute accuracy of the predictions. T.E.S.T. determines the AD by analyzing the structural similarity between the compound to be predicted and the compounds in the training dataset. If a compound is outside the AD, the reliability of the prediction will be significantly reduced. T.E.S.T. provides an AD index so that users can evaluate the reliability of each specific prediction. To enhance the reliability of the results, T.E.S.T. also provides information about similar compounds in the database and their experimental LD50 values. This allows users to qualitatively assess the plausibility of predictions based on the structural similarity and toxicity of known compounds. This method is particularly useful in the early screening stages of drug development, helping to reduce the number of animal tests and optimize research resources.

3. RESULTS AND DISCUSSION

3.1. Results of molecular docking simulation

3.1.1. Docking energy

Table 2 recorded the docking energy of 13 aromatic compounds which is reported to exist in cinnamomi ramulus essential oil, and 3 references: acarbose, voglibose và miglitol. These compounds are docked into

the binding sites of AA (4W93) and AG (5NN4), respectively. Considering the 4W93 receptor, the docking energies of the 13 aromatic compounds ranged from -4.425 kcal/mol to -6.819 kcal/mol. Of these, benzyl benzoate recorded the lowest docking energy of -6.819 kcal/mol, followed by 1-naphthalenol and transanethole with docking energies of -5.952 kcal/mol and -5.668 kcal/mol, correspondingly. The docking energies of the top 3 compounds were much higher than that of acarbose, with a value of -7.973 kcal/mol, and were also close to the energy of miglitol, which was -5.776 kcal/mol, and lower than voglibose, -4.996 kcal/mol. Other compounds with docking energies lower than 5 kcal/mol include 1-phenyl-1,2-propanedione, 1-methylethylbenzene, phenylethyl alcohol, phenylpropanal, acetophenone, 2-methylbenzaldehyde, and 3-methylbenzaldehyde, may also have potential uses voglibose. The remaining compounds, hydroxybenzaldehyde, benzaldehyde, and anisole, have higher docking energies than voglibose approximately 0.1 kcal/mol to 0.5 kcal/mol. Since the difference is not large, these last three compounds should still be considered as potential candidates for 4W93 receptor inhibition.

In the case of the 5NN4 receptor, the docking energy values of 13 aromatic compounds and 3 references are recorded in the last column of Table 2. We can immediately see that the benzyl benzoate compound leads among the investigated compounds with a docking energy value of -6.897 kcal/mol. This value is lower than that of all 3 reference substances. Next are 1-phenyl-1,2propanedione, 1-naphthalenol, 1-methylethylbenzene and trans-anethole with docking energies of -5.338 kcal/mol, -5.161 kcal/mol, -5.123 kcal/mol and -5.029 kcal/mol, proportionately. The remaining compounds all have docking energies ranging from lower than -4.2 kcal/mol to higher than -5 kcal/mol. For the 5NN4 receptor, all aromatic compounds examined had lower docking energies than voglibose, -4.266 kcal/mol. This suggests that all 13 compounds could potentially replace voglibose as inhibitors for the 5NN4 receptor. On both enzymes, the binding sites of the three reference drugs and the 13 compounds under investigation were comparatively comparable (see Figure 3 and Figure 4). Benzyl benzoate showed excellent results in docking simulations, always being the leading compound in terms of docking energy at both 4W93 and 5NN4 receptors. Compared to the docking results of acarbose, benzyl benzoate showed better interaction with the 5NN4 receptor. Compared to the other two control compounds, voglibose and miglitol, benzyl benzoate was superior in interacting with both enzymes. This suggests that benzyl benzoate could be a potential inhibitor that could inhibit two enzymes at the same time.

Table 2: Summary of docking energies of 13 considered aromatic compounds and 3 references: acarbose, voglibose, miglitol, which in complexes with α-amylase 4W93 receptor and α-glucosidase 5NN4 receptor.

NT.	Common 1	Docking energy (kcal/mol)					
No.	Compound	4W93 receptor	5NN4 receptor				
1	4-hydroxybenzaldehyde	-4.870	-4.289				
2	Benzaldehyde	-4.682	-4.396				
3	Acetophenone	-5.043	-4.876				
4	Anisole	-4.425	-4.510				
5	3-phenylpropanal	-5.129	-4.754				
6	Benzyl benzoate	-6.819	-6.897				
7	2-methylbenzaldehyde	-5.029	-4.423				
8	3-methylbenzaldehyde	-5.018	-4.907				
9	Phenylethyl alcohol	-5.292	-4.850				
10	1-phenyl-1,2-propanedione	-5.482	-5.338				
11	1-naphthalenol	-5.952	-5.161				
12	1-methylethylbenzene	-5.261	-5.123				
13	trans-anethole	-5.668	-5.029				
14	Acarbose	-7.973	-6.705				
15	Voglibose	-4.996	-4.266				
16	Miglitol	-5.776	-5.963				

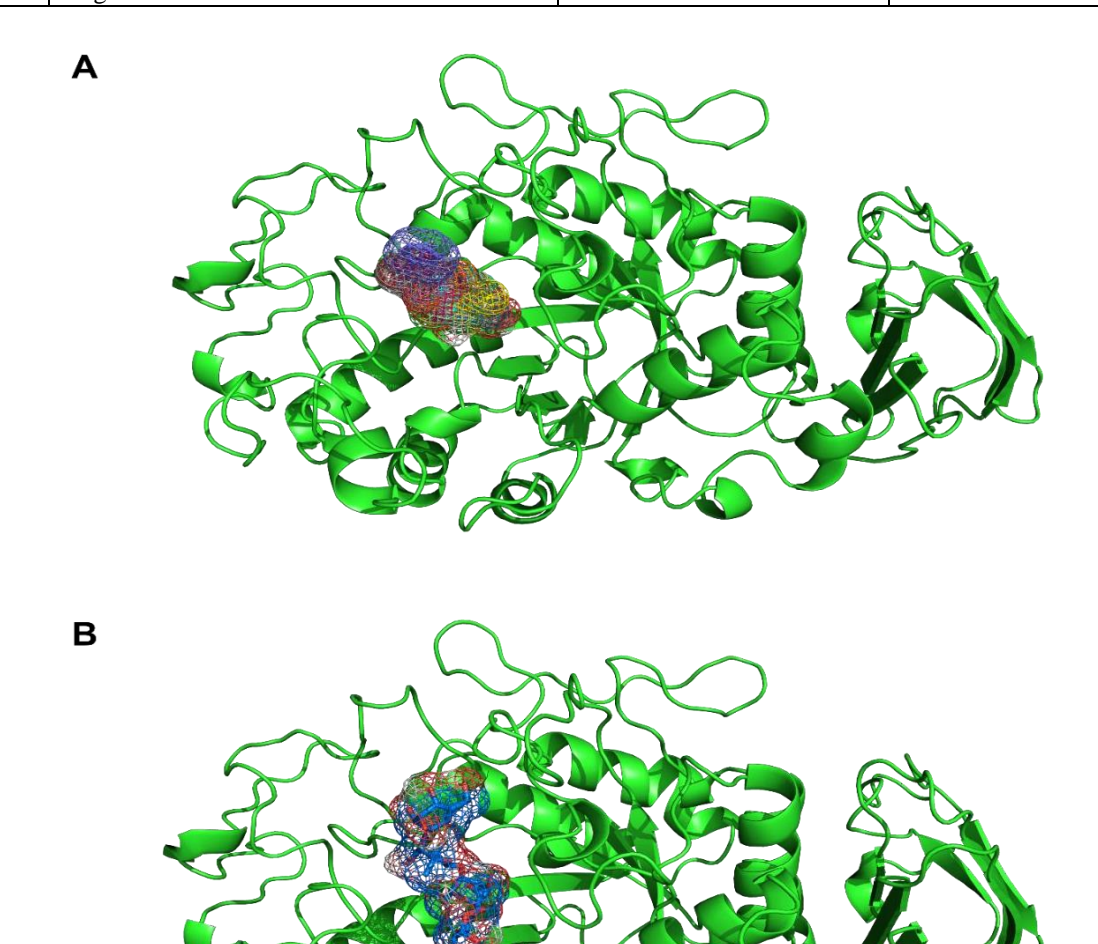


Figure 3: Docking position of compounds in AA receptor (4W93). (A) Position of 13 considered aromatic compounds (colorful mesh). (B) Position of acarbose (blue-red mesh).

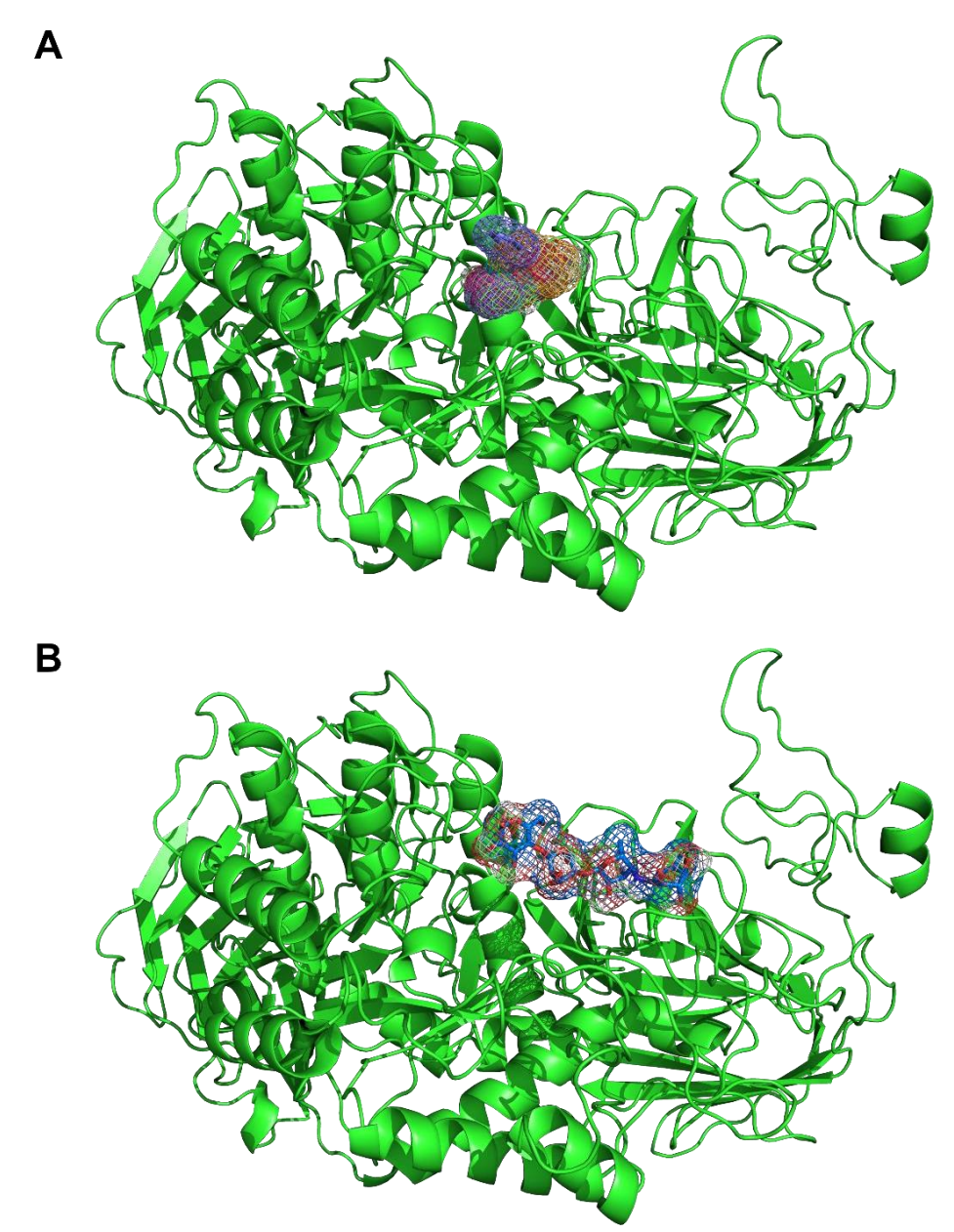


Figure 4: Docking position of compounds in AG receptor (5NN4). (A) Position of 13 considered aromatic compounds (colorful mesh). (B) Position of acarbose (blue-red mesh).

3.1.2. Protein-ligand interaction analysis

Table 3, four types of interactions between the 13 aromatic compounds and the 3 reference compounds with the 4W93 receptor are presented. We can immediately see that hydrophobic interactions are the dominant interactions in the 13 complexes between the 4W93 receptor and the aromatic compounds. Specifically, a total of 9 out of 13 compounds have hydrophobic interactions accounting for 80% or more of the total interactions, see Figure 5. Among them, the compound 1-methylethylbenzene even shows only hydrophobic interactions with the 4W93 receptor. The main residues involved in hydrophobic interactions with these compounds include Trp58, Trp59, Tyr62 and Leu165. These are all residues with hydrophobic side chains. Besides hydrophobic interactions, most of these aromatic compounds also form at least 1 hydrogen bond with the receptor such as 4-hydroxybenzaldehyde (4

bonds), 3-methylbenzaldehyde (2 bonds), phenylethyl alcohol (2 bonds)... Residues Gln63, Arg195 and His299 are the 3 residues that contribute to forming hydrogen bonds with the aromatic compounds surveyed. 1naphthalenol and 1-methylethylbenzene are compounds that do not form hydrogen bonds with the 4W93 receptor. In addition, the four compounds 4hydroxybenzaldehyde, benzyl benzoate, methylbenzaldehyde and 1-naphthalenol show π stacking interactions with residues Trp59 and Tyr62 at the active site of the 4W93 receptor. In another direction, the three reference substances, including acarbose, voglibose and miglitol, showed hydrogen bonding with the 4W93 receptor as the main one, accounting for more than 90% of the total interactions/bindings, see Figure 5. In addition, miglitol formed a salt bridge with residue

Asp197 at the active site of the 4W93 receptor, detailed in Table S1.

Table 4 shows the number of four types of interactions/bindings between the 5NN4 receptor with the 13 aromatic compounds examined and the three references. In general, similar to the complexes with the receptor, hydrophobic interactions also predominate in this case. A total of 12/13 aromatic compounds have more than 50% hydrophobic interactions out of the total interactions of each complex. Residues Trp376, Ile441, Trp481, Trp516, Trp613, and Leu677 frequently participate in Phe649 hydrophobic interactions with the 13 aromatic compounds examined. In addition to benzyl benzoate, 1methylethylbenzene and trans-anethole, the remaining compounds form hydrogen bonds with residues such as Trp481, Asp518, Arg600 and His674. Notably, residue Trp481 is also the only residue that shows π -stacking interactions with some of the aromatic compounds examined. Furthermore, we can see that benzyl benzoate forms a salt bridge with residue Arg600. Similar to the case of the 4W93 receptor, the reference substances mainly form hydrogen bonds with the 5NN4 receptor, the number of hydrogen bonds is up to 11 with the acarbose compound, 6 with the voglibose compound and 5 with the miglitol compound. In addition, voglibose also forms a salt bridge with residue Asp282 of the 5NN4 receptor. (See detail in Table S2)

When analyzing the interactions between the compounds with the two enzymes, we also noted the interaction mechanisms of the investigated compounds and the substances. While the reference substances inhibit the two receptors through interactions with the active site mainly by hydrogen bonding, the investigated aromatic group interacts with the receptor mainly by hydrophobic interactions, some of which also show π -stacking interactions. This indicates to the writers the cause of the adverse effects of the current medications.

However, further research is still needed to understand and confirm this.

Figure 7, Figure S1 and S2 illustrate the key molecular interactions between ligands and amino acids in the receptor binding site. In terms of spatial structure, the interactions analyzed through the PLIP program all follow the rules of optimal distance and bond angle. In panel A, the π -stacking interaction between the aromatic rings of benzyl benzoate with Trp58 and Trp59 shows the parallel arrangement of the π systems, an important feature in stabilizing the protein-ligand complex. In panel B, the network of hydrophobic and hydrogen bond interactions creates a binding environment with optimized entropy and enthalpy. This is described by the arrangement of amino acids such as Leu677, Phe649, and Arg600 around the ligand. The structures of acarbose in panels C and D show high conformational adaptability. This is demonstrated by its ability to interact at multiple points with many different amino acids. Of particular importance is the difference in interaction patterns between AA (4W93) and AG (5NN4). This difference reflects the selectivity of the binding pocket and has important implications for structure-based drug design (SBDD). In panel D, the presence of a salt bridge (shown as the yellow line with yellow spheres at both ends) indicates that an ion-ion interaction contributes to the orientation and stabilization of the complex. Hydrophobic interactions (dashed lines) play an important role in removing water molecules from the binding pocket, resulting in an entropic effect that favors binding. At the same time, the hydrogen bond network (dark blue lines) provides specificity and directionality for binding. This result has important implications for understanding molecular interaction mechanisms and can be applied in the optimization of new molecular dopants. Understanding these interaction patterns can also be applied to molecular docking methods and molecular dynamics simulations.

Table 3: Summary table of the interactions between AA receptor and studied compounds after molecular docking simulation.

	simuuton.							
No.	Compound	Hydrophobic interaction	Hydrogen bond	π-stacking	Salt bridge			
1	4-hydroxybenzaldehyde	2	4	1	-			
2	Benzaldehyde	4	1	-	-			
3	Acetophenone	6	1	-	-			
4	Anisole	4	1	-	-			
5	3-phenylpropanal	6	1	-	-			
6	Benzyl benzoate	2	1	3	-			
7	2-methylbenzaldehyde	6	1	-	-			
8	3-methylbenzaldehyde	3	2	1	-			
9	Phenylethyl alcohol	4	2	-	-			
10	1-phenyl-1,2-propanedione	6	1	-	-			
11	1-naphthalenol	4	-	1	-			
12	1-methylethylbenzene	4	-	-	-			
13	trans-anethole	7	1	-	-			
14	Acarbose	1	6	-	-			
15	Voglibose	1	5	=	-			
16	Miglitol	-	5	-	1			

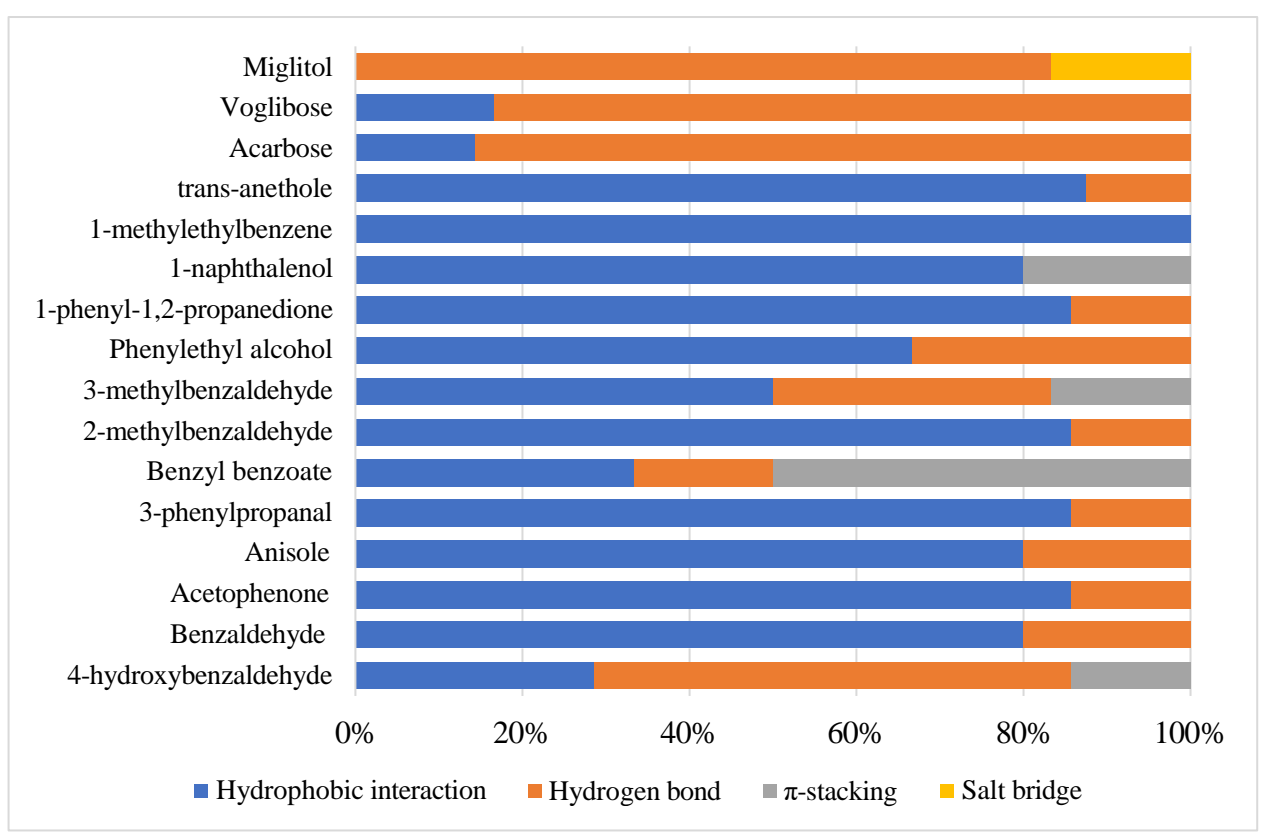


Figure 5: Contributions of interactions in the complex between the 4W93 receptor and the investigated compounds.

Table 4: Summary table of the interactions between AG receptor and studied compounds after molecular docking simulation.

		Similatio			
No.	Compound	Hydrophobic interaction	Hydrogen bond	π-stacking	Salt bridge
1	4-hydroxybenzaldehyde	3	1	-	-
2	Benzaldehyde	5	1	-	-
3	Acetophenone	1	1	-	-
4	Anisole	5	1	-	-
5	3-phenylpropanal	3	1	1	-
6	Benzyl benzoate	9	-	-	1
7	2-methylbenzaldehyde	4	1	1	-
8	3-methylbenzaldehyde	4	1	-	-
9	Phenylethyl alcohol	3	1	1	-
10	1-phenyl-1,2-propanedione	3	2	1	-
11	1-naphthalenol	2	2	2	-
12	1-methylethylbenzene	4	-	1	-
13	trans-anethole	3	-	1	-
14	Acarbose	1	11	-	-
15	Voglibose	-	6	-	1
16	Miglitol	-	5	-	-

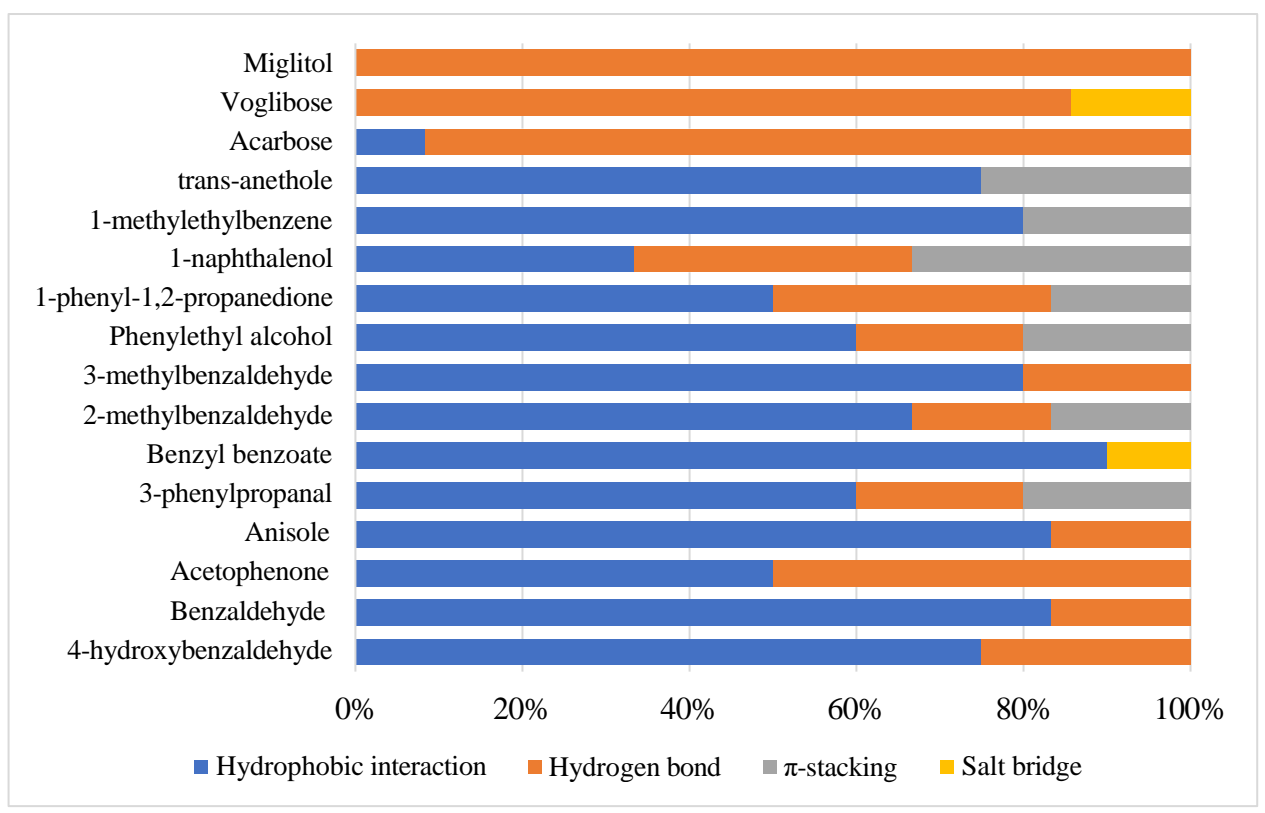


Figure 6: Contributions of interactions in the complex between the 5NN4 receptor and the investigated compounds.

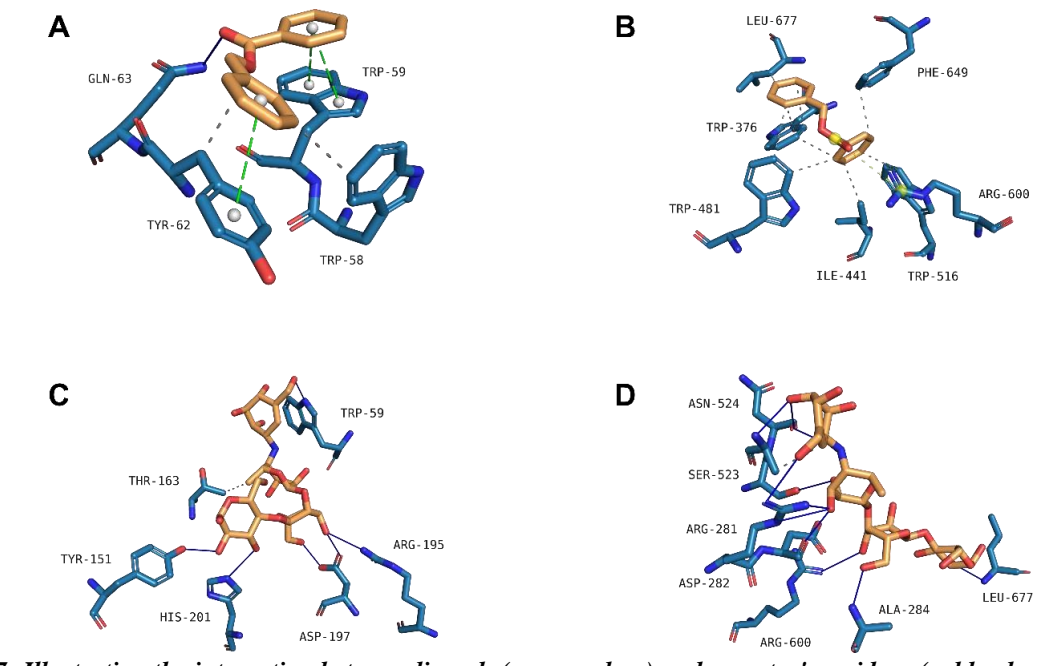


Figure 7: Illustration the interaction between ligands (warm colors) and receptor's residues (cold colors). (A) Benzyl benzoate in interaction with the residues of AA (4W93), (B) benzyl benzoate in interaction with the residues of AG (5NN4), (C) acarbose in interaction with the residues of AA (4W93), (D) acarbose in interaction with the residues of AG (5NN4). Dashed line represents a hydrophobic interaction, dark blue line is hydrogen bond, green dashed line with white spheres at both ends represents a π -stacking interaction, yellow dashed line with yellow spheres at both ends is salt bridge.

3.2. Pharmacokinetic results

3.2.1. Lipophilicity assessment

Table 5 presents the Log $P_{o/w}$ (octanol-water partition coefficient) values of the 13 aromatic compounds studied, predicted by five different methods (iLOGP,

XLOGP3, WLOGP, MLOGP and SILICOS-IT) and the mean value (Consensus). Log $P_{\text{o/w}}$ is an important parameter in pharmaceutical chemistry, which indicates the distribution of the drug between the oil (lipid) and

water phases. The higher the Log Po/w value, the more hydrophobic (lipophilic) the compound is.

From the table, we can see that benzyl benzoate has the highest Log $P_{o/w}$ value (Consensus = 3.25), which is consistent with its structure having two aromatic rings linked together via an ester group. This high hydrophobicity also corresponds to the strong binding energies we saw in the previous docking table (-6.819 and -6.897 kcal/mol). On the other hand, 4hydroxybenzaldehyde has the lowest Log $P_{o/w}$ value (Consensus = 1.17), possibly due to the presence of the hydroxyl group (-OH) which increases hydrophilicity of the molecule. This is also reflected in its relatively weak binding energies (-4.870 and -4.289 kcal/mol). Compounds with similar structures often have similar Log $P_{o/w}$ values. For example, 2methylbenzaldehyde and 3-methylbenzaldehyde have

average Log $P_{\text{O/w}}$ values of 1.99 and 1.93, respectively. This shows that the position of the methyl group substituent does not significantly affect the hydrophobicity of the molecule. Comparing the prediction methods, we see that SILICOS-IT often gives higher values than the other methods, while iLOGP often gives lower values. This emphasizes the importance of using multiple prediction methods and taking the average value to get more reliable results.

Combining lipophilicity information with previous docking data, we can see a correlation between compounds with high Log $P_{\text{O/W}}$ (such as benzyl benzoate) generally having stronger binding energies. This suggests that hydrophobic interactions may play an important role in the binding of compounds to the receptor.

Table 5: Summary table of lipophilicity indices of 13 aromatic compounds investigated. The Log $P_{O/W}$ results obtained from the Swiss ADME server were estimated using 5 methods (iLOGP, XLOGP3, WLOGP, MLOGP and SILICOS-IT) and are presented in the first 5 columns of the Log $P_{O/W}$ field, the last column is the average value of all 5 methods.

	Command	$\operatorname{Log} P_{o/\!w}$							
No.	Compound	iLOGP	XLOGP3	WLOGP	MLOGP	SILICOS-IT	Consensus		
1	4-hydroxybenzaldehyde	0.99	1.35	1.2	0.79	1.52	1.17		
2	Benzaldehyde	1.36	1.48	1.5	1.45	2.05	1.57		
3	Acetophenone	1.64	1.58	1.89	1.78	2.19	1.82		
4	Anisole	1.88	2.11	1.7	1.81	1.89	1.88		
5	3-phenylpropanal	1.68	1.3	1.82	2.1	2.66	1.91		
6	Benzyl benzoate	2.68	3.97	2.89	3.41	3.29	3.25		
7	2-methylbenzaldehyde	1.63	2.26	1.81	1.78	2.47	1.99		
8	3-methylbenzaldehyde	1.63	1.95	1.81	1.78	2.47	1.93		
9	Phenylethyl alcohol	1.7	1.36	1.22	1.87	2.03	1.64		
10	1-phenyl-1,2-propanedione	1.01	1.72	1.46	1.08	2.03	1.46		
11	1-naphthalenol	1.67	2.85	2.55	2.54	2.54	2.43		
12	1-methylethylbenzene	2.25	3.66	2.81	4.17	2.83	3.14		
13	trans-anethole	2.55	3.3	2.62	2.67	2.79	2.79		

3.2.2. Water solubility index evaluation

Table 6 presents the Log S (water solubility) values of compounds, predicted by three different methods: ESOL, Ali and SILICOS-IT. Log S is an important parameter indicating the solubility of a compound in water. Looking at the Log S values, we can see that all the compounds have negative values, indicating relatively low solubility in water. The more negative the value, the lower the solubility. 4-hydroxybenzaldehyde and phenylethyl alcohol have relatively better solubility than the other compounds, which can be explained by the presence of the hydroxyl group (-OH) in their structures. In contrast, benzyl benzoate shows the lowest solubility, with Log S values ranging from -3.95 to -5.01 depending on the prediction method. This is consistent

with its molecular structure, which consists of two aromatic rings and a highly hydrophobic ester group. Structurally similar compounds such as 2-methylbenzaldehyde and 3-methylbenzaldehyde have quite close Log S values, indicating that the position of the methyl group substituent does not greatly affect the solubility of the molecule.

Comparing the three prediction methods, SILICOS-IT generally gives more negative values (lower solubility) than the other two methods. This is particularly evident for compounds such as benzyl benzoate and 3-phenylpropanal. Meanwhile, the Ali method generally gives less negative values, suggesting a higher solubility prediction.

Table 6: Summary table of water solubility indices of 13 aromatic compounds investigated. The Log S results obtained from the SwissADME server were estimated using three methods including ESOL, Ali and SILICOS-IT.

NT.	G	$\log S$					
No.	Compound	ESOL	Ali	SILICOS-IT			
1	4-hydroxybenzaldehyde	-1.87	-1.74	-1.72			
2	Benzaldehyde	-1.92	-1.45	-2.28			
3	Acetophenone	-2.01	-1.55	-2.68			
4	Anisole	-2.33	-1.93	-2.46			
5	3-phenylpropanal	-1.74	-1.26	-3.12			
6	Benzyl benzoate	-3.95	-4.22	-5.01			
7	2-methylbenzaldehyde	-2.44	-2.25	-2.68			
8	3-methylbenzaldehyde	-2.24	-1.93	-2.68			
9	Phenylethyl alcohol	-1.82	-1.39	-2.58			
10	1-phenyl-1,2-propanedione	-2.11	-2.05	-2.66			
11	1-naphthalenol	-3.2	-2.93	-3.47			
12	1-methylethylbenzene	-3.32	-3.35	-3.17			
13	trans-anethole	-3.11	-3.17	-2.98			

3.2.3. Evaluation of pharmacokinetic parameter

Table 7 presents several properties of the 13 investigated compounds, focusing on their pharmacokinetic parameters and interactions with metabolizing enzymes. The structural diversity of the 13 compounds, including aldehydes, alcohols and benzene derivatives, allows for the assessment of the influence of different functional groups on pharmacokinetic properties. These data are of great value in assessing the pharmacokinetic potential of compounds, especially in the field of drug development and safety assessment of chemical compounds. Selected enzyme interaction models also provide useful information on potential drug interactions and the main metabolic pathways of these compounds.

Most of the compounds (12/13) showed high absorption via the gastrointestinal tract, except for 1-methylethyl benzene, which was the only compound with low absorption among the investigated compounds. This suggests that the structural features of most of these compounds favor gastrointestinal absorption, which may be related to their lipid solubility and suitable molecular size. In addition, the good gastrointestinal absorption of most of the above compounds suggests that they have good oral bioavailability, an important characteristic for orally administered drugs. All compounds were able to cross the blood-brain barrier, which is important for assessing the potential neuroactive effects of the investigated compounds, as

well as their potential use in the treatment of diseases related to the central nervous system. This property can be an advantage or a disadvantage depending on the therapeutic target. If the target is to act on the central nervous system, this is a beneficial property. Conversely, if this effect is not targeted, it can lead to unwanted side effects.

Regarding interactions with P-glycoprotein, the investigated compounds were all determined not to be substrates of the P-glycoprotein receptor. This is significant because P-glycoprotein is a transport protein that can push drugs out of cells, reducing the bioavailability and therapeutic efficacy of the compounds. Concerning interactions with CYP450 enzymes, the data indicate a selective interaction pattern with CYP450 isoforms. The majority of compounds are predicted to interact with CYP1A19. In particular, benzyl benzoate has also been shown to interact with CYP2C9. This should be noted as it may lead to undesirable drug-drug interactions with other drugs metabolized by these enzymes.

The Log K_p (skin permeability coefficient) values ranged from -6.20 cm/s to -4.43 cm/s. These values indicate that the compounds have different skin permeability abilities, with 1-methylethyl benzene having the highest permeability (Log $K_p = -4.43$ cm/s) and 3-phenylpropanal having the lowest permeability (Log $K_p = -6.20$ cm/s).

Table7: Summary table of some pharmacokinetic indicators of 13 aromatic compounds investigated. The indicators include absorption through the digestive tract; permeability through the blood-brain barrier; assessment of whether the investigated compound is a substrate of the P-gp receptor; ability to inhibit drug-interacting enzymes: CYP1A2,

	C1F2C19, C1F2C9, C1F2D0, C1F3A4; and permeability inrough the skin.									
No.	Compound	GI absorption	BBB permeant	P-gp substrate	CYP1A2 inhibitor	CYP2C19 inhibitor	CYP2C9 inhibitor	CYP2D6 inhibitor	CYP3A4 inhibitor	Skin permeation Log K_p (cm/s)
1	4- hydroxybenzaldehyde	High	Yes	No	No	No	No	No	No	-6.09
2	Benzaldehyde	High	Yes	No	Yes	No	No	No	No	-5.9
3	Acetophenone	High	Yes	No	Yes	No	No	No	No	-5.91
4	Anisole	High	Yes	No	Yes	No	No	No	No	-5.46
5	3-phenylpropanal	High	Yes	No	Yes	No	No	No	No	-6.20
6	Benzyl benzoate	High	Yes	No	Yes	Yes	No	No	No	-4.78

7	2- methylbenzaldehyde	High	Yes	No	Yes	No	No	No	No	-5.43
8	3- methylbenzaldehyde	High	Yes	No	Yes	No	No	No	No	-5.65
9	Phenylethyl alcohol	High	Yes	No	Yes	No	No	No	No	-6.08
10	1-phenyl-1,2- propanedione	High	Yes	No	Yes	No	No	No	No	-5.98
11	1-naphthalenol	High	Yes	No	Yes	No	No	No	No	-5.16
12	1-methylethylbenzene	Low	Yes	No	No	No	No	No	No	-4.43
13	trans-anethole	High	Yes	No	Yes	No	No	No	No	-4.86

3.2.4. Evaluating drug-likeness rules

Table 8 provides information on drug-likeness properties according to different sets of criteria (Lipinski, Ghose, Veber, Egan, and Muegge) as well as predicted bioavailability values of the compounds. These rules are important criteria used in the early stages of drug development to evaluate the absorption and distribution of potential molecules. The Lipinski rules[70, 71] set thresholds for molecular weight, lipid solubility (LogP), and the number of hydrogen bond donors/acceptors. The Ghose rules[72] add criteria for the number of atoms and rings in the molecule. The Veber rules[73] focus on the mobility of the molecule through the number of rotatable bonds and surface polarity. The Egan rules[74] focus on the ability to penetrate biological membranes, while the Muegge rules[75] provide a comprehensive set of criteria that incorporates many factors. Although these rules are useful in initial screening and saving research costs, they should be applied flexibly and in conjunction with other assessments, as many successful drugs on the market may still violate some of the criteria in these rules.

With respect to drug rule violations, the data show that most compounds comply with these rules quite well. Specifically, only 1-methylethylbenzene violates the Lipinski rule with 1 violation, related to MLOGP value (> 4.15), while the remaining compounds do not violate this rule. The Ghose rule appears to be more stringent, with many compounds having a high number of violations (up to 3 violations) such as 4-

hydroxybenzaldehyde, benzaldehyde, acetophenone, anisole, 2-methylbenzaldehyde, 3-methylbenzaldehyde, and phenylethyl alcohol. Violations are mainly related to molecular weight (<160 g/mol), molar refractivity (<40), and atomic number less than 20 atoms. Some other compounds have fewer violations (1 or 2 violations), and only benzyl benzoate does not violate any of the criteria in this rule. It is noteworthy that none of the compounds violated the Veber and Egan rules, indicating that these compounds have physical-chemical properties that conform to the criteria of these two rules. Regarding the Muegge rule, most of the compounds had 1-2 violations, mainly related to molecular weight (<200 g/mol); benzyl benzoate alone had no violations. This further confirms that benzvl benzoate is the compound with the best medicinal properties among the studied

Regarding bioavailability values, all compounds were predicted to have similar values of 0.55, indicating that they have moderate systemic absorption. This is consistent with their physical-chemical properties as seen in the previous tables for lipid solubility and water solubility.

Overall, benzyl benzoate emerged as the compound with the best drug-likeness properties with the least violations. This, combined with the good binding energy from the previous docking results, further confirms the potential of benzyl benzoate in drug development in order to inhibit α -amylase and α -glucosidase.

Table 8: Summary table of 5 sets of drug-likeness assessment criteria and bioavailability scores of 13 surveyed aromatic compounds.

No.	Compound	Lipinski violation	Ghose violation	Veber violation	Egan violation	Muegge violation	Bioavailability
1	4-hydroxybenzaldehyde	0	3	0	0	1	0.55
2	Benzaldehyde	0	3	0	0	2	0.55
3	Acetophenone	0	3	0	0	2	0.55
4	Anisole	0	3	0	0	2	0.55
5	3-phenylpropanal	0	1	0	0	2	0.55
6	Benzyl benzoate	0	0	0	0	0	0.55
7	2-methylbenzaldehyde	0	3	0	0	2	0.55
8	3-methylbenzaldehyde	0	3	0	0	2	0.55
9	Phenylethyl alcohol	0	3	0	0	2	0.55
10	1-phenyl-1,2-propanedione	0	2	0	0	1	0.55
11	1-naphthalenol	0	2	0	0	2	0.55
12	1-methylethylbenzene	1	1	0	0	2	0.55
13	trans-anethole	0	1	0	0	2	0.55

3.2.5. Assessment of medicinal chemical properties Table 9 provides information on the toxicity warnings and druggability of compounds through four important

parameters: PAINS alerts, Brenk alerts, leadlikeness, and synthetic accessibility. Regarding PAINS (Pan-Assay Interference Compounds) alerts, most compounds

have no warnings, except for 1-phenyl-1,2-propanedione, which has one (imine_one_A). This hints that these compounds are less likely to interfere in biological assays, an important characteristic in drug development.

There is a clear separation between the compounds when we consider the Brenk alert. Some compounds such as 4-hvdroxybenzaldehvde. benzaldehvde methylbenzaldehyde derivatives have an alert, while the remaining compounds do not have any one. The Brenk warnings relate to functional groups that may be toxic or unstable in the body. Specifically, this is the presence of in the aldehyde group compounds: hydroxybenzaldehyde, benzaldehyde, 3phenylpropanal, 2-methylbenzaldehyde 3methylbenzaldehyde; and the diketo group in 1-phenyl-1,2-propanedione.

It is noteworthy that the leadlikeness values of benzyl benzoate and 1-methylethylbenzene have higher values (=2) than the other compounds (=1). This suggests that these two compounds have more suitable properties for development as lead compounds. In terms of synthetic accessibility, most of the compounds have a value of 1, except for benzyl benzoate (=1.44) and trans-anethole (=1.47), which have higher values. This advocates that these two compounds may be more complex to synthesize, but are still within acceptable limits.

Combined with the data from the previous tables, benzyl benzoate continues to appear to be a promising candidate. Despite its more complex synthesis than the other compounds, it has no toxicological warnings and a good leadlikeness profile. This, together with the good binding energy and favorable pharmacokinetic properties seen previously, further confirms the potential of benzyl benzoate for drug development supporting diabetes treatment.

Table 9: Summary table of medicinal chemical properties of 13 aromatic compounds investigated.

No.	Compound	PAINS alert	Brenk alert	Leadlikeness	Synthetic accessibility
1	4-hydroxybenzaldehyde	0	1	1	1
2	Benzaldehyde	0	1	1	1
3	Acetophenone	0	0	1	1
4	Anisole	0	0	1	1
5	3-phenylpropanal	0	1	1	1
6	Benzyl benzoate	0	0	2	1.44
7	2-methylbenzaldehyde	0	1	1	1
8	3-methylbenzaldehyde	0	1	1	1
9	Phenylethyl alcohol	0	0	1	1
10	1-phenyl-1,2-propanedione	1	1	1	1
11	1-naphthalenol	0	0	1	1
12	1-methylethylbenzene	0	0	2	1
13	trans-anethole	0	0	1	1.47

3.3. Results of acute toxicity LD50

Table 10 contains information on the acute toxicity (LD50) values of the compounds, including both experimental values and values predicted by using T.E.S.T. software. For the reference substances, acarbose and voglibose showed low toxicity with experimental LD50 of 23989.66 mg/kg and 20000.07 mg/kg, respectively. Miglitol has no experimental value but is predicted to have an LD50 of 19414.07 mg/kg. These values tell us that the reference drugs have a high safety profile. Compared with the reference substances, the test compounds were generally significantly more toxic. The compound acetophenone showed the highest toxicity with an experimental LD50 of 814.25 mg/kg, approximately 29 times lower than that of acarbose. In contrast, anisole had the lowest toxicity among the tested compounds with an experimental LD50 of 3698.51 mg/kg but was still significantly lower than that of the

references. Notably, benzyl benzoate, which had shown good pharmacokinetic properties and binding energy in previous analyses, had an experimental LD50 of 1900.50 mg/kg. Although its toxicity was higher than that of the references, this value was still within the acceptable range for drug development.

When comparing the experimental and predicted values, some significant differences can be seen. For example, acarbose has a predicted value (11477.03 mg/kg) that is much lower than the experimental value (23989.66 mg/kg). 4-hydroxybenzaldehyde, anisole, 1-naphthalenol and voglibose are also predicted to have lower LD50 values than experimentally. Meanwhile, acetophenone, benzyl benzoate, phenylethyl alcohol and 1-methylethylbenzene are the opposite of the above case. This highlights the importance of performing realistic toxicity tests during the drug investigation.

Table 10: Summary table of experimental and and predicted LD50 values of 13 aromatic compounds examined and 3 reference compounds: acarbose, voglibose and miglitol.

	rejerence compounds, acuroose, rogioose and miguoi.							
No.	Compound	Experimental LD50 (mg/kg)	Predicted LD50 (mg/kg)					
1	4-hydroxybenzaldehyde	2248.13	1153.97					
2	Benzaldehyde	1299.69	1284.68					
3	Acetophenone	814.25	1511.06					
4	Anisole	3698.51	1042.07					
5	3-phenylpropanal	-	2202.56					
6	Benzyl benzoate	1900.50	3284.97					
7	2-methylbenzaldehyde	-	1372.36					
8	3-methylbenzaldehyde	-	1175.43					
9	Phenylethyl alcohol	1790.61	2308.20					
10	1-phenyl-1,2-propanedione	-	2076.74					
11	1-naphthalenol	1870.27	1144.58					
12	1-methylethylbenzene	1399.40	3374.08					
13	trans-anethole	2088.85	2140.97					
14	Acarbose	23989.66	11477.03					
15	Voglibose	20000.07	10788.96					
16	Miglitol	-	19414.07					

4. CONCLUSION

This research provides several significant findings regarding the potential of aromatic compounds from ramulus cinnamomi as dual inhibitors of α -amylase and α-glucosidase. The molecular docking studies revealed that benzyl benzoate exhibits exceptional binding affinities to both AA (-6.819 kcal/mol) and AG (-6.897 kcal/mol) enzymes, surpassing most reference compounds. This dual inhibitory potential suggests it could be a promising lead compound for diabetes treatment. The interaction analysis uncovered a distinct binding mechanism for the aromatic compounds, primarily through hydrophobic interactions, compared to the hydrogen bond-dominated binding of current drugs. This difference in binding mechanisms could potentially lead to reduced side effects and improved therapeutic outcomes. Pharmacokinetic analyses demonstrated that most compounds, particularly benzyl benzoate, possess favorable drug-like properties including high gastrointestinal absorption and ability to cross the blood-brain barrier. While the compounds showed higher acute toxicity compared to reference drugs, their LD50 values remained within acceptable ranges for therapeutic development.

The scientific significance of this work lies in identifying novel natural compounds with dual enzyme inhibitory potential and elucidating their unique binding mechanisms. These findings contribute to our understanding of structure-activity relationships in enzvme inhibition and natural product drug development. For future research, we recommend conducting in vitro and in vivo studies to validate the predicted inhibitory effects and investigate potential synergistic effects between these compounds. Simultaneously we focus on developing structural modifications to optimize the binding properties while reducing toxicity and exploring the relationship between hydrophobic binding mechanisms and reduced side effects. Finally, we also try performing molecular dynamics simulations to better understand the stability and kinetics of these interactions.

REFFERENCE

- 1. International Diabetes Federation. IDF Diabetes Atlas, 10th edn. Brussels, Belgium: 2021. Available at: https://www.diabetesatlas.org.
- Fryirs, M., Barter, P. J., and Rye, K. A., Cholesterol metabolism and pancreatic beta-cell function. Curr Opin Lipidol, 2009. 20(3): p. 159-64.
- 3. Bailey, C. J. and Turner, R. C., *Metformin*. N Engl J Med, 1996. **334**(9): p. 574-9.
- 4. Tomlinson, B., Patil, N. G., Fok, M., Chan, P., and Lam, C. W. K., *The role of sulfonylureas in the treatment of type 2 diabetes*. Expert Opin Pharmacother, 2022. **23**(3): p. 387-403.
- Dahlen, A. D., Dashi, G., Maslov, I., Attwood, M. M., Jonsson, J., Trukhan, V., and Schioth, H. B., Trends in Antidiabetic Drug Discovery: FDA Approved Drugs, New Drugs in Clinical Trials and Global Sales. Front Pharmacol, 2021. 12: p. 807548.
- 6. Ahren, B., *DPP-4 inhibitors*. Best Pract Res Clin Endocrinol Metab, 2007. **21**(4): p. 517-33.
- 7. Aschner, P., Kipnes, M. S., Lunceford, J. K., Sanchez, M., Mickel, C., Williams-Herman, D. E., and Sitagliptin Study, G., Effect of the dipeptidyl peptidase-4 inhibitor sitagliptin as monotherapy on glycemic control in patients with type 2 diabetes. Diabetes Care, 2006. **29**(12): p. 2632-7.
- Augeri, D. J., Robl, J. A., Betebenner, D. A., Magnin, D. R., Khanna, A., Robertson, J. G., Wang, A., Simpkins, L. M., Taunk, P., Huang, Q., Han, S. P., Abboa-Offei, B., Cap, M., Xin, L., Tao, L., Tozzo, E., Welzel, G. E., Egan, D. M., Marcinkeviciene, J., Chang, S. Y., Biller, S. A., Kirby, M. S., Parker, R. A., and Hamann, L. G., Discovery and preclinical profile of Saxagliptin (BMS-477118): a highly potent, long-acting, orally active dipeptidyl peptidase IV inhibitor for the treatment of type 2 diabetes. J Med Chem, 2005. 48(15): p. 5025-37.
- 9. Eckhardt, M., Klein, T., Nar, H., and Thiemann, S., Discovery of Linagliptin for the Treatment of Type 2 Diabetes Mellitus. 2015: p. 129-156.

- 10. DeFronzo, R. A., Fleck, P. R., Wilson, C. A., Mekki, Q., and Alogliptin Study, G., Efficacy and safety of the dipeptidyl peptidase-4 inhibitor alogliptin in patients with type 2 diabetes and inadequate glycemic control: a randomized, double-blind, placebo-controlled study. Diabetes Care, 2008. 31(12): p. 2315-7.
- 11. Drucker, D. J., Dritselis, A., and Kirkpatrick, P., *Liraglutide*. Nat Rev Drug Discov, 2010. **9**(4): p. 267-8.
- 12. Marso, S. P., Bain, S. C., Consoli, A., Eliaschewitz, F. G., Jodar, E., Leiter, L. A., Lingvay, I., Rosenstock, J., Seufert, J., Warren, M. L., Woo, V., Hansen, O., Holst, A. G., Pettersson, J., Vilsboll, T., and Investigators, S.-. Semaglutide and Cardiovascular Outcomes in Patients with Type 2 Diabetes. N Engl J Med, 2016. 375(19): p. 1834-1844.
- 13. Umpierrez, G., Tofe Povedano, S., Perez Manghi, F., Shurzinske, L., and Pechtner, V., Efficacy and safety of dulaglutide monotherapy versus metformin in type 2 diabetes in a randomized controlled trial (AWARD-3). Diabetes Care, 2014. 37(8): p. 2168-76.
- 14. Frias, J. P., Davies, M. J., Rosenstock, J., Perez Manghi, F. C., Fernandez Lando, L., Bergman, B. K., Liu, B., Cui, X., Brown, K., and Investigators, S.-. *Tirzepatide versus Semaglutide Once Weekly in Patients with Type 2 Diabetes.* N Engl J Med, 2021. **385**(6): p. 503-515.
- 15. Plosker, G. L., *Dapagliflozin: a review of its use in type 2 diabetes mellitus*. Drugs, 2012. **72**(17): p. 2289-312.
- Neal, B., Perkovic, V., Mahaffey, K. W., de Zeeuw, D., Fulcher, G., Erondu, N., Shaw, W., Law, G., Desai, M., Matthews, D. R., and Group, C. P. C., Canagliflozin and Cardiovascular and Renal Events in Type 2 Diabetes. N Engl J Med, 2017. 377(7): p. 644-657.
- 17. Zinman, B., Wanner, C., Lachin, J. M., Fitchett, D., Bluhmki, E., Hantel, S., Mattheus, M., Devins, T., Johansen, O. E., Woerle, H. J., Broedl, U. C., Inzucchi, S. E., and Investigators, E.-R. O., Empagliflozin, Cardiovascular Outcomes, and Mortality in Type 2 Diabetes. N Engl J Med, 2015. 373(22): p. 2117-28.
- 18. Marrs, J. C. and Anderson, S. L., *Ertugliflozin in the treatment of type 2 diabetes mellitus*. Drugs Context, 2020. **9**.
- 19. Agrawal, N., Sharma, M., Singh, S., and Goyal, A., *Recent Advances of alpha-Glucosidase Inhibitors: A Comprehensive Review.* Curr Top Med Chem, 2022. **22**(25): p. 2069-2086.
- 20. Kaur, N., Kumar, V., Nayak, S. K., Wadhwa, P., Kaur, P., and Sahu, S. K., *Alpha-amylase as molecular target for treatment of diabetes mellitus: A comprehensive review.* Chem Biol Drug Des, 2021. **98**(4): p. 539-560.
- 21. Khan, F., Khan, M. V., Kumar, A., and Akhtar, S., Recent Advances in the Development of Alpha-Glucosidase and Alpha-Amylase Inhibitors in Type 2 Diabetes Management: Insights from In silico to In vitro Studies. Curr Drug Targets, 2024.

- 22. Whitcomb, D. C. and Lowe, M. E., *Human pancreatic digestive enzymes*. Dig Dis Sci, 2007. **52**(1): p. 1-17.
- 23. Asano, N., *Glycosidase inhibitors: update and perspectives on practical use.* Glycobiology, 2003. **13**(10): p. 93R-104R.
- 24. Kumar, S., Narwal, S., Kumar, V., and Prakash, O., alpha-glucosidase inhibitors from plants: A natural approach to treat diabetes. Pharmacogn Rev, 2011. 5(9): p. 19-29.
- 25. Sales, P. M., Souza, P. M., Simeoni, L. A., and Silveira, D., alpha-Amylase inhibitors: a review of raw material and isolated compounds from plant source. J Pharm Pharm Sci, 2012. **15**(1): p. 141-83.
- 26. Chen, L., Sun, P., Wang, T., Chen, K., Jia, Q., Wang, H., and Li, Y., Diverse mechanisms of antidiabetic effects of the different procyanidin oligomer types of two different cinnamon species on db/db mice. J Agric Food Chem, 2012. 60(36): p. 9144-50.
- 27. Kawamura-Konishi, Y., Watanabe, N., Saito, M., Nakajima, N., Sakaki, T., Katayama, T., and Enomoto, T., Isolation of a new phlorotannin, a potent inhibitor of carbohydrate-hydrolyzing enzymes, from the brown alga Sargassum patens. J Agric Food Chem, 2012. **60**(22): p. 5565-70.
- 28. Martin, A. E. and Montgomery, P. A., *Acarbose: an alpha-glucosidase inhibitor*. Am J Health Syst Pharm, 1996. **53**(19): p. 2277-90; quiz 2336-7.
- 29. Vichayanrat, A., Ploybutr, S., Tunlakit, M., and Watanakejorn, P., Efficacy and safety of voglibose in comparison with acarbose in type 2 diabetic patients. Diabetes Res Clin Pract, 2002. 55(2): p. 99-103.
- 30. van de Laar, F. A., Lucassen, P. L., Akkermans, R. P., van de Lisdonk, E. H., Rutten, G. E., and van Weel, C., Alpha-glucosidase inhibitors for patients with type 2 diabetes: results from a Cochrane systematic review and meta-analysis. Diabetes Care, 2005. 28(1): p. 154-63.
- 31. Lam, T. P., Tran, N. N., Pham, L. D., Lai, N. V., Dang, B. N., Truong, N. N., Nguyen-Vo, S. K., Hoang, T. L., Mai, T. T., and Tran, T. D., Flavonoids as dual-target inhibitors against alpha-glucosidase and alpha-amylase: a systematic review of in vitro studies. Nat Prod Bioprospect, 2024. 14(1): p. 4.
- 32. Prpa, E. J., Bajka, B. H., Ellis, P. R., Butterworth, P. J., Corpe, C. P., and Hall, W. L., A systematic review of in vitro studies evaluating the inhibitory effects of polyphenol-rich fruit extracts on carbohydrate digestive enzymes activity: a focus on culinary fruits consumed in Europe. Crit Rev Food Sci Nutr, 2021. 61(22): p. 3783-3803.
- 33. Farazi, M., Houghton, M. J., Cardoso, B. R., Murray, M., and Williamson, G., *Inhibitory effect of extracts from edible parts of nuts on alpha-amylase activity: a systematic review.* Food Funct, 2024. **15**(10): p. 5209-5223.
- 34. Xiao, J., Ni, X., Kai, G., and Chen, X., A review on structure-activity relationship of dietary polyphenols inhibiting alpha-amylase. Crit Rev Food Sci Nutr, 2013. **53**(5): p. 497-506.

- 35. Li, K., Yao, F., Xue, Q., Fan, H., Yang, L., Li, X., Sun, L., and Liu, Y., Inhibitory effects against alphaglucosidase and alpha-amylase of the flavonoidsrich extract from Scutellaria baicalensis shoots and interpretation of structure-activity relationship of its eight flavonoids by a refined assign-score method. Chem Cent J, 2018. 12(1): p. 82.
- 36. Proenca, C., Freitas, M., Ribeiro, D., Oliveira, E. F. T., Sousa, J. L. C., Tome, S. M., Ramos, M. J., Silva, A. M. S., Fernandes, P. A., and Fernandes, E., alpha-Glucosidase inhibition by flavonoids: an in vitro and in silico structure-activity relationship study. J Enzyme Inhib Med Chem, 2017. 32(1): p. 1216-1228.
- 37. Medagama, A. B., The glycaemic outcomes of Cinnamon, a review of the experimental evidence and clinical trials. Nutr J, 2015. 14: p. 108.
- 38. Ranasinghe, P., Pigera, S., Premakumara, G. A., Galappaththy, P., Constantine, G. R., and Katulanda, P., *Medicinal properties of 'true' cinnamon (Cinnamomum zeylanicum): a systematic review.*BMC Complement Altern Med, 2013. **13**: p. 275.
- 39. Allen, R. W., Schwartzman, E., Baker, W. L., Coleman, C. I., and Phung, O. J., *Cinnamon use in type 2 diabetes: an updated systematic review and meta-analysis.* Ann Fam Med, 2013. **11**(5): p. 452-9.
- 40. Davis, P. A. and Yokoyama, W., *Cinnamon intake lowers fasting blood glucose: meta-analysis.* J Med Food, 2011. **14**(9): p. 884-9.
- 41. Zhu, R., Liu, H., Liu, C., Wang, L., Ma, R., Chen, B., Li, L., Niu, J., Fu, M., Zhang, D., and Gao, S., *Cinnamaldehyde in diabetes: A review of pharmacology, pharmacokinetics and safety.* Pharmacol Res, 2017. **122**: p. 78-89.
- 42. Sahni, T., Sharma, S., Verma, D., and Kaur, P., *Overview of Coumarins and its Derivatives: Synthesis and Biological Activity.* Letters in Organic Chemistry, 2021. **18**(11): p. 880-902.
- 43. Kumari, S., Saini, R., Bhatnagar, A., and Mishra, A., Exploring plant-based alpha-glucosidase inhibitors: promising contenders for combatting type-2 diabetes. Arch Physiol Biochem, 2024. **130**(6): p. 694-709.
- 44. Wang, H., Du, Y.-J., and Song, H.-C., α-Glucosidase and α-amylase inhibitory activities of guava leaves. Food Chemistry, 2010. **123**(1): p. 6-13.
- 45. Ogboye, R. M., Patil, R. B., Famuyiwa, S. O., and Faloye, K. O., *Novel alpha-amylase and alpha-glucosidase inhibitors from selected Nigerian antidiabetic plants: an in silico approach.* J Biomol Struct Dyn, 2022. **40**(14): p. 6340-6349.
- 46. Sharma, P., Joshi, T., Joshi, T., Chandra, S., and Tamta, S., Molecular dynamics simulation for screening phytochemicals as alpha-amylase inhibitors from medicinal plants. J Biomol Struct Dyn, 2021. 39(17): p. 6524-6538.
- 47. Riyaphan, J., Pham, D. C., Leong, M. K., and Weng, C. F., In Silico Approaches to Identify Polyphenol Compounds as alpha-Glucosidase and alpha-Amylase Inhibitors against Type-II Diabetes. Biomolecules, 2021. 11(12).

- 48. Liu, J., Zhang, Q., Li, R. L., Wei, S. J., Huang, C. Y., Gao, Y. X., and Pu, X. F., *The traditional uses, phytochemistry, pharmacology and toxicology of Cinnamomi ramulus: a review.* J Pharm Pharmacol, 2020. **72**(3): p. 319-342.
- 49. Huang, D. F., Xu, J. G., Liu, J. X., Zhang, H., and Hu, Q. P., Chemical constituents, antibacterial activity and mechanism of action of the essential oil from Cinnamomum cassia bark against four foodrelated bacteria. Microbiology, 2014. 83(4): p. 357-365.
- 50. Li, Y.-q., Kong, D.-x., and Wu, H., *Analysis and evaluation of essential oil components of cinnamon barks using GC–MS and FTIR spectroscopy.* Industrial Crops and Products, 2013. **41**: p. 269-278.
- 51. Berman, H. M., Westbrook, J., Feng, Z., Gilliland, G., Bhat, T. N., Weissig, H., Shindyalov, I. N., and Bourne, P. E., *The Protein Data Bank*. Nucleic Acids Res, 2000. **28**(1): p. 235-42.
- 52. Burley, S. K., Bhikadiya, C., Bi, C., Bittrich, S., Chao, H., Chen, L., Craig, P. A., Crichlow, G. V., Dalenberg, K., Duarte, J. M., Dutta, S., Fayazi, M., Feng, Z., Flatt, J. W., Ganesan, S., Ghosh, S., Goodsell, D. S., Green, R. K., Guranovic, V., Henry, J., Hudson, B. P., Khokhriakov, I., Lawson, C. L., Liang, Y., Lowe, R., Peisach, E., Persikova, I., Piehl, D. W., Rose, Y., Sali, A., Segura, J., Sekharan, M., Shao, C., Vallat, B., Voigt, M., Webb, B., Westbrook, J. D., Whetstone, S., Young, J. Y., Zalevsky, A., and Zardecki, C., RCSB Protein Data Bank (RCSB.org): delivery experimentally-determined structures alongside one million computed structure proteins models from of artificial intelligence/machine learning. Nucleic Acids Res, 2023. **51**(D1): p. D488-D508.
- 53. Williams, L. K., Zhang, X., Caner, S., Tysoe, C., Nguyen, N. T., Wicki, J., Williams, D. E., Coleman, J., McNeill, J. H., Yuen, V., Andersen, R. J., Withers, S. G., and Brayer, G. D., *The amylase inhibitor* montbretin A reveals a new glycosidase inhibition motif. Nat Chem Biol, 2015. 11(9): p. 691-6.
- 54. Brayer, G. D., Luo, Y., and Withers, S. G., *The structure of human pancreatic alpha-amylase at 1.8 A resolution and comparisons with related enzymes.* Protein Sci, 1995. **4**(9): p. 1730-42.
- 55. van der Maarel, M. J., van der Veen, B., Uitdehaag, J. C., Leemhuis, H., and Dijkhuizen, L., Properties and applications of starch-converting enzymes of the alpha-amylase family. J Biotechnol, 2002. 94(2): p. 137-55.
- 56. Roig-Zamboni, V., Cobucci-Ponzano, B., Iacono, R., Ferrara, M. C., Germany, S., Bourne, Y., Parenti, G., Moracci, M., and Sulzenbacher, G., Structure of human lysosomal acid alpha-glucosidase-a guide for the treatment of Pompe disease. Nat Commun, 2017. 8(1): p. 1111.
- 57. Sugawara, K., Saito, S., Sekijima, M., Ohno, K., Tajima, Y., Kroos, M. A., Reuser, A. J., and Sakuraba, H., Structural modeling of mutant alphaglucosidases resulting in a processing/transport defect in Pompe disease. J Hum Genet, 2009. 54(6): p. 324-30.

- 58. Kishnani, P. S. and Howell, R. R., *Pompe disease in infants and children*. J Pediatr, 2004. **144**(5 Suppl): p. S35-43.
- 59. Khalid, H., Butt, M. H., ur Rehman Aziz, A., Ahmad, I., Iqbal, F., Shamim, A., Nishan, U., Ullah, R., Ibrahim, M. A., Moura, A. A., Shah, M., and Sun, W., Phytobioinformatics screening of ayurvedic plants for potential α-glucosidase inhibitors in diabetes management. Current Plant Biology, 2024. 40: p. 100404.
- 60. Maulana, A. F., Sriwidodo, S., Rukayadi, Y., and Maksum, I. P., In Silico Study of Mangostin Compounds and Its Derivatives as Inhibitors of alpha-Glucosidase Enzymes for Anti-Diabetic Studies. Biology (Basel), 2022. 11(12).
- 61. Sanner, M. F., *Python: a programming language for software integration and development.* J Mol Graph Model, 1999. **17**(1): p. 57-61.
- 62. Eberhardt, J., Santos-Martins, D., Tillack, A. F., and Forli, S., *AutoDock Vina 1.2.0: New Docking Methods, Expanded Force Field, and Python Bindings.* J Chem Inf Model, 2021. **61**(8): p. 3891-3898.
- 63. Trott, O. and Olson, A. J., AutoDock Vina: improving the speed and accuracy of docking with a new scoring function, efficient optimization, and multithreading. J Comput Chem, 2010. **31**(2): p. 455-61.
- 64. Salentin, S., Schreiber, S., Haupt, V. J., Adasme, M. F., and Schroeder, M., *PLIP: fully automated protein-ligand interaction profiler*. Nucleic Acids Res, 2015. **43**(W1): p. W443-7.
- 65. Adasme, M. F., Linnemann, K. L., Bolz, S. N., Kaiser, F., Salentin, S., Haupt, V. J., and Schroeder, M., *PLIP 2021: expanding the scope of the proteinligand interaction profiler to DNA and RNA*. Nucleic Acids Res, 2021. **49**(W1): p. W530-W534.
- 66. Schrodinger, LLC, *The PyMOL Molecular Graphics System, Version 1.8.* 2015.

- 67. Daina, A., Michielin, O., and Zoete, V., SwissADME: a free web tool to evaluate pharmacokinetics, druglikeness and medicinal chemistry friendliness of small molecules. Sci Rep, 2017. 7: p. 42717.
- 68. Daina, A. and Zoete, V., A BOILED-Egg To Predict Gastrointestinal Absorption and Brain Penetration of Small Molecules. ChemMedChem, 2016. **11**(11): p. 1117-21.
- 69. Zhu, H., Martin, T. M., Ye, L., Sedykh, A., Young, D. M., and Tropsha, A., *Quantitative structure-activity relationship modeling of rat acute toxicity by oral exposure*. Chem Res Toxicol, 2009. **22**(12): p. 1913-21.
- 70. Lipinski, C. Computational alerts for potential absorption problems: profiles of clinically tested drugs. in Tools for Oral Absorption. Part Two. Predicting Human Absorption. BIOTEC, PDD symposium, AAPS, Miami. 1995.
- 71. Lipinski, C. A., Lombardo, F., Dominy, B. W., and Feeney, P. J., Experimental and computational approaches to estimate solubility and permeability in drug discovery and development settings. Advanced Drug Delivery Reviews, 2012. **64**: p. 4-17.
- 72. Ghose, A. K., Viswanadhan, V. N., and Wendoloski, J. J., A knowledge-based approach in designing combinatorial or medicinal chemistry libraries for drug discovery. 1. A qualitative and quantitative characterization of known drug databases. J Comb Chem, 1999. 1(1): p. 55-68.
- Veber, D. F., Johnson, S. R., Cheng, H. Y., Smith, B. R., Ward, K. W., and Kopple, K. D., Molecular properties that influence the oral bioavailability of drug candidates. J Med Chem, 2002. 45(12): p. 2615-23.
- 74. Egan, W. J., Merz, K. M., Jr., and Baldwin, J. J., *Prediction of drug absorption using multivariate statistics*. J Med Chem, 2000. **43**(21): p. 3867-77.
- 75. Muegge, I., Heald, S. L., and Brittelli, D., *Simple selection criteria for drug-like chemical matter.* J Med Chem, 2001. **44**(12): p. 1841-6.

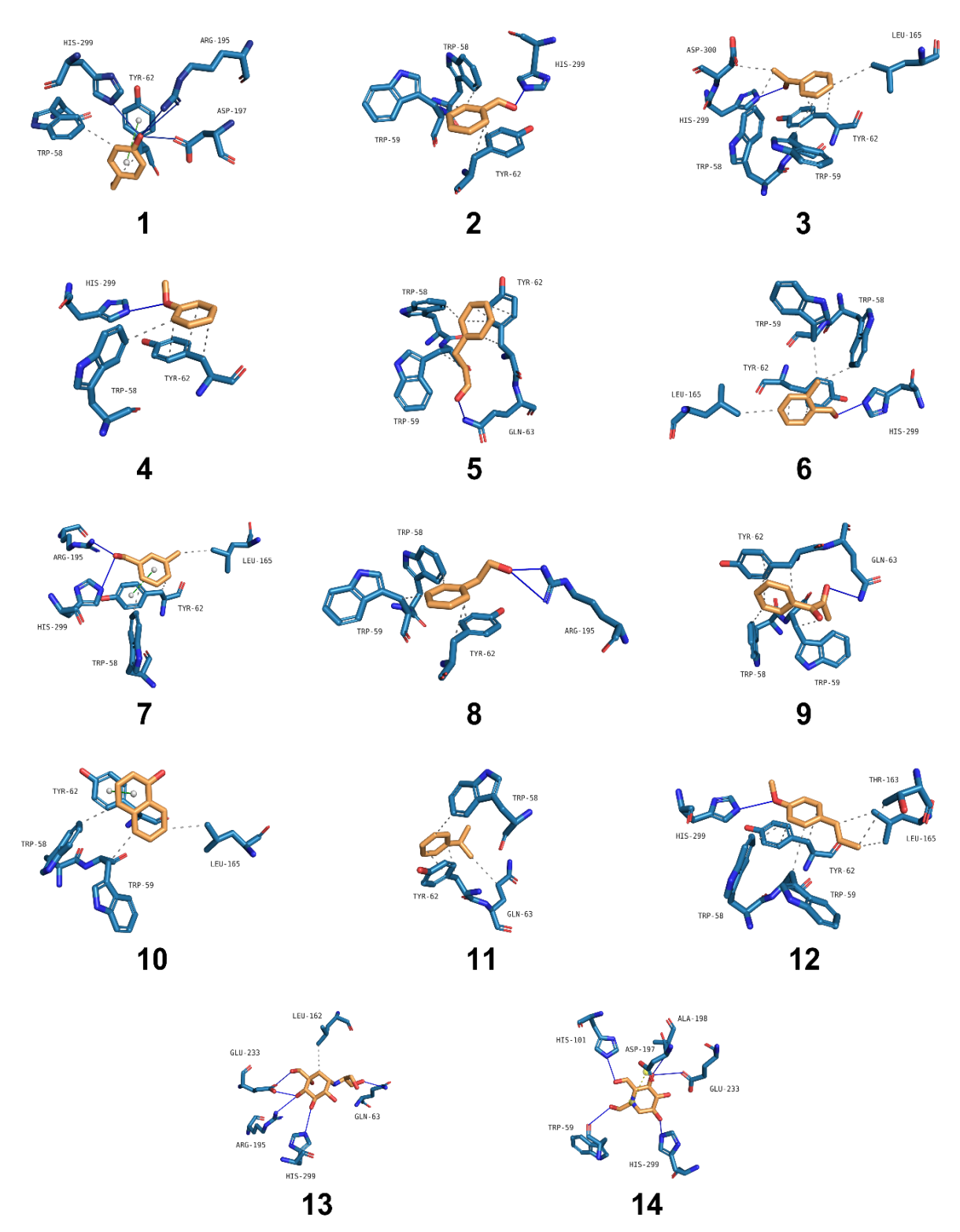


Figure S1: Illustration the interaction between ligands (warm colors) and AA receptor's residues (cold colors). (1) 4-hydroxybenzaldehyde, (2) benzaldehyde, (3) acetophenone, (4) anisole, (5) 3-phenylpropanal, (6) 2-methylbenzaldehyde, (7) 3-methylbenzaldehyde, (8) phenylethyl alcohol, (9) 1-phenyl-1,2-propanedione, (10) 1-naphthalenol, (11) 1-methylethylbenzene, (12) trans-anethole, (13) voglibose, (14) miglitol. Dashed line represents a hydrophobic interaction, dark blue line is hydrogen bond, green dashed line with white spheres at both ends represents a π-stacking interaction, yellow dashed line with yellow spheres at both ends is salt bridge.

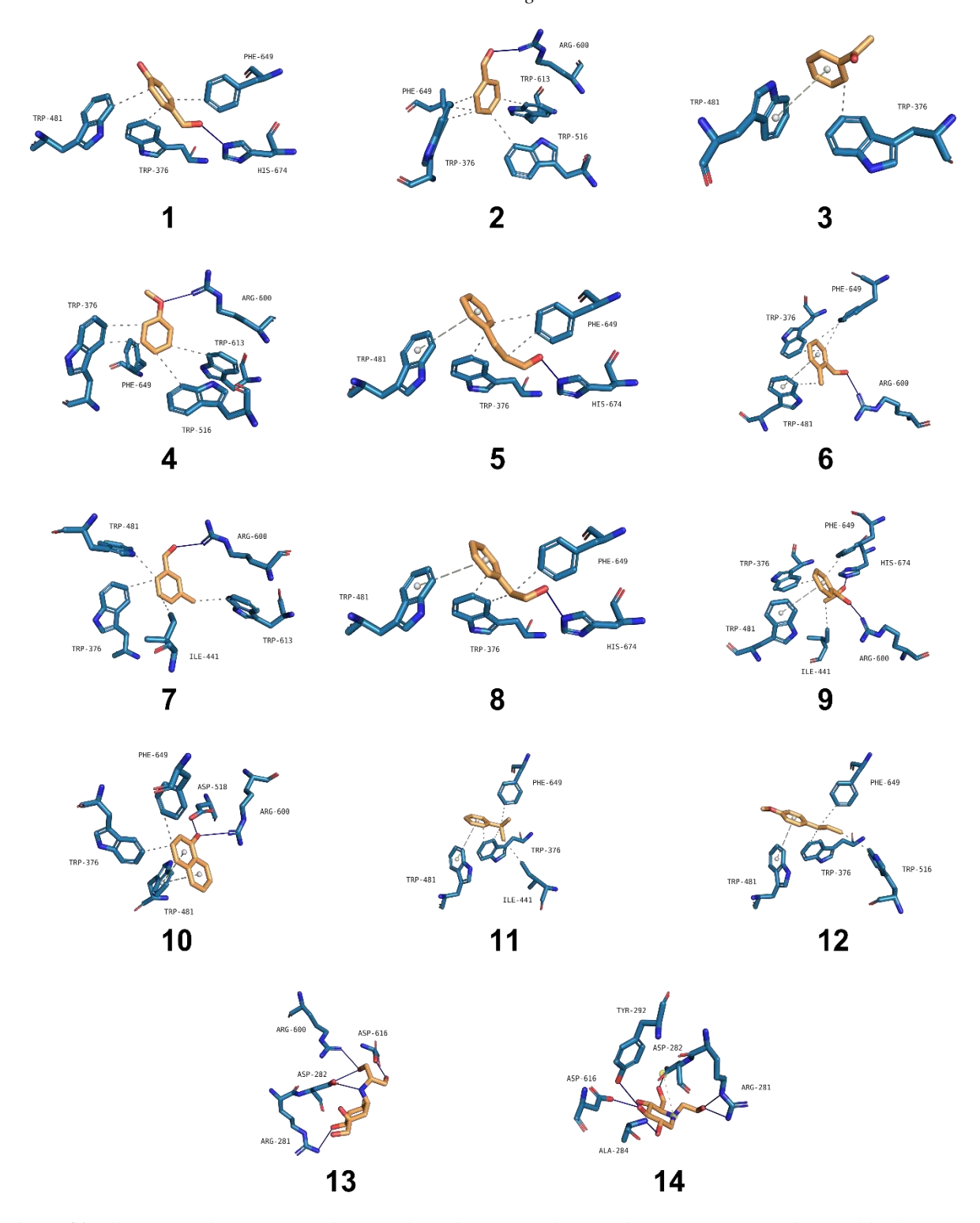


Figure S2: Illustration the interaction between ligands (warm colors) and AG receptor's residues (cold colors). (1) 4-hydroxybenzaldehyde, (2) benzaldehyde, (3) acetophenone, (4) anisole, (5) 3-phenylpropanal, (6) 2-methylbenzaldehyde, (7) 3-methylbenzaldehyde, (8) phenylethyl alcohol, (9) 1-phenyl-1,2-propanedione, (10) 1-naphthalenol, (11) 1-methylethylbenzene, (12) trans-anethole, (13) voglibose, (14) miglitol. Dashed line represents a hydrophobic interaction, dark blue line is hydrogen bond, green dashed line with white spheres at both ends represents a π-stacking interaction, yellow dashed line with yellow spheres at both ends is salt bridge.

Table S1: List of the interactions of 13 aromatic compounds and 3 reference compounds with the 4W93 receptor. Each value is presented in the format "residue": "bond length/interaction distance".

No.	Compound	Hydrophobic interaction	Hydrogen bond	π-stacking interaction	Salt bridge
1	4-hydroxybenzaldehyde	TRP58: 3.50, TYR62: 3.64	ARG195: 3.84, ARG195: 3.31, ASP197: 2.90, HIS299: 3.36	TYR62: 4.07	
2	Benzaldehyde	TRP58: 3.89, TRP59: 3.72, TYR62: 3.72, TYR62: 3.60	HIS299: 3.10		
3	Acetophenone	TRP58: 3.78, TRP59: 3.71, TYR62: 3.77, TYR62: 3.68, LEU165: 3.88, ASP300: 3.68	HIS299: 2.97		
4	Anisole	TRP58: 3.68, TYR62: 3.82, TYR62: 3.74, TYR62: 3.70	HIS299: 3.21		
5	3-phenylpropanal	TRP58: 3.57, TRP59: 3.73, TYR62: 3.70, TYR62: 3.72, TYR62: 3.66, TYR62: 3.86	GLN63: 3.07		
6	Benzyl benzoate	TRP58: 3.54, TYR62: 3.48	GLN63: 3.04	TRP59: 3.76, TRP59: 3.97, TYR62: 4.31	
7	2-methylbenzaldehyde	TRP58: 3.57, TRP59: 3.57, TYR62: 3.77, TYR62: 3.68, TYR62: 3.76, LEU165: 3.52	HIS299: 2.94		
8	3-methylbenzaldehyde	TRP58: 3.52, TYR62: 3.58, LEU165: 3.60	ARG195: 3.26, HIS299: 3.14	TYR62: 4.24	
9	Phenylethyl alcohol	TRP58: 3.77, TRP59: 3.74, TYR62: 3.67, TYR62: 3.50	ARG195: 2.98, ARG195: 3.90		
10	1-phenyl-1,2-propanedione	TRP58: 3.53, TRP59: 3.71, TYR62: 3.88, TYR62: 3.63, TYR62: 3.69, TYR62: 3.83	GLN63: 3.98		
11	1-naphthalenol	TRP58: 3.43, TRP59: 3.37, TYR62: 3.59, LEU165: 3.56		TYR62: 4.19	
12	1-methylethylbenzene	TRP58: 3.66, TYR62: 3.65, TYR62: 3.62, GLN63: 3.74			
13	trans-anethole	TRP58: 3.57, TRP59: 3.89, TYR62: 3.74,	HIS299: 3.22		

		TYR62: 3.68, THR163: 3.96, LEU165: 3.67, LEU165: 3.71			
14	Acarbose	THR163: 3.60	TRP59: 2.99, TYR151: 2.78, ARG195: 3.27, ASP197: 2.88, ASP197: 2.70, HIS201: 3.20	-	-
15	Voglibose	LEU162: 3.88	GLN63: 3.28, ARG195: 3.28, GLU233: 2.99, GLU233: 3.02, HIS299: 3.12	-	-
16	Miglitol	-	TRP59: 3.67, HIS101: 3.07, ALA198: 3.79, GLU233: 3.56, HIS299: 2.80	-	ASP197: 4.99

Table S2: List of the interactions of 13 aromatic compounds and 3 reference compounds with the 5NN4 receptor. Each value is presented in the format "residue": "bond length/interaction distance".

		Hydrophobic		π-stacking	T
No.	Compound	interaction	Hydrogen bond	interaction	Salt bridge
1	4-hydroxybenzaldehyde	TRP376: 3.48,	HIS674: 3.27		
		TRP481: 3.81,			
		PHE649: 3.39			
		TRP376: 3.47,			
2	Benzaldehyde	TRP376: 3.81,	ARG600: 2.92		
		TRP516: 3.69,			
		TRP613: 3.69,			
		PHE649: 3.60			
3	Acetophenone	TRP376: 3.45	TRP481: 5.21		
		TRP376: 3.69,			
		TRP376: 3.57,			
4	Anisole	TRP516: 3.83,	ARG600: 2.92		
		TRP613: 3.76,			
		PHE649: 3.73			
	3-phenylpropanal	TRP376: 3.58,			
5		PHE649: 3.72,	HIS674: 3.15	TRP481: 5.14	
		PHE649: 3.88			
	Benzyl benzoate	TRP376: 3.59,			
		TRP376: 3.66,			
		TRP376: 3.34,			
		ILE441: 3.81,			
6		TRP481: 3.66,			ARG600: 5.44
		TRP481: 3.66,			
		TRP516: 3.83,			
		PHE649: 3.68,			
		LEU677: 3.99			
7	2-methylbenzaldehyde	TRP376: 3.59,			
		TRP481: 3.77,	ARG600: 2.95	TRP481: 5.26	
		PHE649: 3.67,	AKG000. 2.93		
		PHE649: 3.72			
8	3-methylbenzaldehyde	TRP376: 3.34,	ARG600: 2.85		
		ILE441: 3.84,			
		TRP481: 3.61,			
		TRP613: 3.68			
9	Phenylethyl alcohol	TRP376: 3.42,	HIS674: 3.22	TRP481: 5.28	
	I helly lettly 1 dicollor	TRP376: 3.87,	111007 1. 3.22	1101. 5.20	

The Ability To Inhibit A-Amylase And A-Glucosidase By Aromatic Compounds In Cinnamomi Ramulus Extract: An In Silico Investigation

		PHE649: 3.53			
10	1-phenyl-1,2- propanedione	TRP376: 3.62, ILE441: 3.92, PHE649: 3.67	ARG600: 2.95, HIS674: 3.34	TRP481: 5.10	
11	1-naphthalenol	TRP376: 3.48, PHE649: 3.43	ASP518: 3.09, ARG600: 3.02	TRP481: 4.91, TRP481: 5.26	
12	1-methylethylbenzene	TRP376: 3.51, TRP376: 3.96, ILE441: 3.86, PHE649: 3.71		TRP481: 5.20	
13	trans-anethole	TRP376: 3.63, TRP516: 3.70, PHE649: 3.89		TRP481: 5.01	
14	Acarbose	ALA555: 3.59	ARG281: 3.21, ARG281: 3.44, ARG281: 2.97, ASP282: 2.69, ALA284: 3.18, SER523: 3.61, ASN524: 4.05, ASN524: 4.06, ALA555: 2.96, ARG600: 3.52, LEU677: 3.64		-
15	Voglibose	-	ARG281: 3.52, ARG281: 3.15, ASP282: 2.85, ALA284: 2.91, TYR292: 4.02, ASP616: 3.10		ASP282: 4.32
16	Miglitol	-	ARG281: 4.03, ASP282: 3.55, ASP282: 3.22, ARG600: 2.91, ASP616: 3.19		-